MINI-SUPERCELL EVENT OF 23 OCTOBER 2004 IN THE MEMPHIS COUNTY WARNING AREA

Jonathan L. Howell* and Jason F. Beaman
National Weather Service Forecast Office
Memphis, Tennessee

August 15, 2006

1. INTRODUCTION

Low-topped supercell thunderstorms developed on 23 October 2004 and moved over portions of the Memphis County Warning Area (CWA)(west Tennessee and north Mississippi). These thunderstorms produced one tornado, several funnel clouds, and areas of severe straight-line wind damage. The most significant damage occurred when a tornado moved through the community of Marianna in Marshall County, Mississippi. The tornadic damage was rated F1 on the Fujita scale and produced a 70 m wide swath of damage along a 4.8 km long path (Fig. 1). One home in the region sustained significant roof damage (Fig. 2), two trailer homes were damaged, and many large trees were snapped and uprooted (Fig. 3). This tornado was spawned by one of the low-topped supercell thunderstorms that developed.

These thunderstorms exhibited *mini-supercell* characteristics with storm echo tops averaging between 7-11 km (Burgess et. al., 1995)(Gerard et. al., 2000), small significant echo diameters (Kennedy et. al., 1993), and strong rotation through a significant portion of the thunderstorm updraft column (Markowski and Straka, 2000). The atmospheric conditions in areas where these mini-supercells developed exhibited limited thermodynamic instability and moderate amounts of low-level environmental shear.

Atmospheric environments that support development of mini-supercells are uncommon across the Mid-South, yet are most likely to occur during the cool season. Most tornadoes that form over this portion of the country are produced by typical supercell thunderstorms. Typical supercell thunderstorms have significant echo tops in excess of 12 km (Wicker et al., 1996), possess much larger significant echo diameters, and exhibit strong, deep rotation to significant heights in the atmosphere. In addition, typical supercell thunderstorms form in environments that exhibit moderate to strong instability and high shear.

This case study will investigate the near storm environment that favored mini-supercell thunderstorm development over the Mid-South. In addition, a radar analysis will be performed to identify storm structures associated with the mini-supercell thunderstorms that developed. These analyses will be used to (1) provide diagnosis of mini-supercell structure and threats, (2) assist warning meteorologists in identifying environments favorable for low-topped convection, and (3) provide evidence of and impacts from storm-scale boundary interactions and their effects on miniature supercells. It is the authors overall intent to provide information that will assist meteorologists in properly warning for low-topped convection in the southern United States.

2. PRE-STORM ENVIRONMENT

a. Surface Conditions

Regional surface observations at 1200 UTC, 23 October 2004, indicated a strong 988 mb low pressure system positioned over southern Minnesota with a weak warm front that extended southeast across the lower Great Lakes through the Ohio Valley (Fig. 4). An outflow boundary (referred to hereafter as Convective Outflow Boundary #1) from overnight convection also extended across east Arkansas into northwest Mississippi at 1400 UTC (Fig. 5). Along and to the southwest of this outflow boundary, an unstable airmass existed with southwest surface winds, temperatures ranging from 21°C to 23°C, and dewpoint temperatures approaching 21°C. Areas located northeast of the boundary were slightly more stable with southeast surface winds, slightly lower temperatures (below 20°C), and lower dewpoint temperatures (less than 19°C).

Surface low pressure continued moving northeast into southern Ontario as Convective Outflow Boundary #1 was forced slowly east by a decaying cold pool. As this convective outflow moved across portions of northwest Mississippi through 1900 UTC, it served as a focusing mechanism for convective development and enhanced low-level vorticity. As thunderstorms developed and propagated northeast across this boundary they acquired low-level rotation and eventually produced well-developed wall clouds and funnel clouds across extreme northwest Mississippi.

Additional thunderstorms developed further southwest along Convective Outflow Boundary #1 prior to 1900 UTC and continued to propagate east along the boundary through 2100 UTC. A second, more subtle, convective outflow boundary (referred to hereafter as Convective Outflow Boundary #2) was generated by discreet convective cells to the southeast of Convective Outflow Boundary #1. Convective Outflow Boundary #2 became the focus for new supercell thunderstorm development and locally enhanced vorticity (Fig. 6).

B. Upper Air Conditions

The upper level environment was also favorable for thunderstorm development over the Mid-South. This was a result of a strengthening low-level jet streak, a well-defined mid-level shortwave trough axis that moved across the region, and favorable positioning under the right entrance region of a strong upper-level jet maximum (Bluestein, 2000). Each of these upper air features contributed to large scale ascent, which enhanced the new thunderstorms that developed after 1500 UTC.

At 1200 UTC, an 850 mb low center was located over southern Minnesota with a trough axis extending southward across the central Plains states into the Arklatex region. An 18 m s^{-1} 850 mb low-level jet maximum extended from eastern Wisconsin through extreme northern Louisiana (Fig. 7).

The 850 mb low-level jet maximum continued to strengthen to 23 m s^{-1} as it progressed eastward over the forecast area through the day. This low-level jet supplied warm, moist, and unstable air into the region and likely helped to maintain the convection that had developed over

the area.

In the middle levels of the atmosphere, a pronounced positively tilted 500 mb shortwave trough axis was observed over the central High Plains (eastern Nebraska southwestward to the Oklahoma and Texas panhandles) at 1200 UTC (Fig 8). As the day progressed, the mid-level shortwave trough axis moved east with the associated cold air aloft overspreading the near surface warm sector. This helped steepen the lapse rates and promote a more favorable environment for the new convection that developed within the warm sector after 1500 UTC.

This new convection was also enhanced by strengthening upper-level wind fields. A 70 m s^{-1} 250 mb jet maximum that was oriented across the Plains states at 1200 UTC, translated east across the Mississippi valley through early afternoon (Fig. 9). By 1800 UTC, the Mid South came under the influence of the right entrance region of the jet maximum and a region of diffluent flow. This assisted in large scale ascent over the region and maintained the convective evolution through the afternoon.

3. SOUNDING INFORMATION

Several considerations were made to determine the most representative soundings since the location of the mini-supercell thunderstorms were over 160 km away from any one RAOB sounding. The Jackson, Mississippi (JAN) and Shreveport, Louisiana (SHV) sounding sites were selected due to their proximity to the approaching upstream upper level shortwave. In addition, the JAN soundings displayed wind fields that matched well with those measured from the KNQA WSR-88D VAD (Vertical Azimuth Display) wind profiler located in Millington, Tennessee. It was determined that these wind fields best represented the actual wind fields observed over north Mississippi. Since the timing of the event (1700-2200 UTC) occurred between synoptic sounding times, an analysis of the 1200 UTC, 23 October 2004 and 0000 UTC, 24 October 2004 JAN and SHV soundings were utilized.

The 1200 UTC, 23 October 2004 JAN sounding (Fig. 10) was analyzed using a modified surface temperature of 23.9°C and a dewpoint temperature of 21.1°C. These values were an average of the 1700 UTC surrounding surface observations and matched closely to the Oxford, MS and Memphis, TN ASOS (Automated Surface Observation System) observations during the onset of the event. After modifying the JAN soundings, it became apparent that the environment exhibited low CAPE values and moderate shear. Surface based CAPE was 774 J kg^{-1} and the lifted index was -1.4°C. Although the equilibrium level was 12.8 km, the effective CAPE was located between 800 mb and 650 mb (1.5-3.8 km) where steeper lapse rates were present. There was also significant warming of the temperature profile at 625 mb or approximately 4.0 km. This suggested that the strongest updraft resided in the small region of high CAPE. Above this unstable layer, the updraft became weaker and was unable to reach the high equilibrium level. These attributes match well with the findings of Davies (1993) in which mini-supercell events occurred with the best CAPE in the lowest 2 to 3 kilometers and overall CAPE values of 500-1000 J kg^{-1}. The 0-3 km storm relative helicity was 187 m^2 s^{-2} and was marginally supportive of rotating updrafts.

The 1200 UTC, 23 October 2004, SHV sounding (Fig. 11) characteristics were similar to those observed from the 1200 UTC, JAN sounding. The sounding indicated two distinct areas where steeper lapse rates were present. The first layer of steeper lapse rates existed between 810 mb and 725 mb (1.9-2.8 km) and exhibited a temperature decline of 7.0°C. Above this unstable layer, the lapse rates became very poor between 725 mb to 670 mb (2.8-3.6 km). Another layer of steep lapse rates existed from 670 mb to 560 mb (3.6-4.9 km) where the temperature decreased 9.0°C over a distance of 1.3 km. The surface based CAPE using the modified surface parcel was 814 J/kg and the lifted index was -3.0°C. The 0-3 km storm relative helicity was 379 $m^2 s^{-2}$ with most of the helicity resulting from speed shear. Very little directional shear was found in the sounding, especially within the critical 0-1 km layer.

The 0000 UTC, 24 October 2004 JAN (Fig. 12) sounding was also modified using a surface temperature of 23.9°C and a dewpoint temperature of 21.1°C. Instability parameters remained weak with a surface based CAPE of 869 J kg^{-1} and a lifted index of -1.8°C. The observed equilibrium level was 11.4 km, which was lower then observed on the 1200 UTC sounding. Steep lapse rates still existed between 925 mb and 775 mb (0.8-2.3 km) and between 630 mb and 525 mb (3.9-5.4 km). These observed lapse rates allowed for greater effective CAPE within these portions of the sounding. Steep lapse rates were also identified from 500 mb (5.8 km) up to the equilibrium level at 250 mb (11.4 km). It is believed that the steep lapse rates above 500 mb were not realized due to the low topped nature of the cells that developed. To help prove this theory, a method was developed by Markowski et al. (2000) to simulate what the realized CAPE was based on the known observed storm echo tops. In our case the highest known echo top was at approximately 10.7 km. Using a best hand drawn estimate, it was determined that there was very little CAPE above 500 mb (5.8 km), with almost all of it confined below 500 mb (5.8 km). The 0-3 km storm relative helicity was 328 $m^2 s^{-2}$ and was sufficient for rotating updrafts.

The 0000 UTC, 24 October 2004 SHV sounding (Fig. 13) exhibited a favorable environment for the development of mini-supercells. Steep lapse rates existed from 850 mb to 700 mb (1.5-3.1 km) and from 630 mb to 400 mb (4.0-7.5 km). A significant inversion existed between these two layers between 700 mb to 630 mb (3.1-4.0 km). Given the presence of this inversion, the strongest updraft likely existed in the area of steep lapse rates from 850 mb to 700 mb. Upon encountering the inversion at 700 mb, it is believed that the updraft significantly decelerated and did not fully realize the second elevated area of steep lapse rates. Using the modified surface parcel, surface base CAPE was calculated to be 996 J/kg, the lifted index was -2.8°C, and the equilibrium level was 12.1 km. The 0-3 km storm relative helicity was 77 $m^2 s^{-2}$ and was not representative of the wind fields across north Mississippi.

In addition, the freezing level was located at 4.6 km at 1200 UTC and 4.4 km at 0000 UTC as recorded from the JAN soundings. The -20°C level existed at 7.8 km at 1200 UTC and 7.7 km at 0000 UTC. Given that the most intense core of the cells was located below 4.6 km, significant portions of the storms remained below the freezing level. Therefore, the ice nuclei production was low and resulted in the lack of lightning production with these storms. The mini-supercell that traversed Tunica and DeSoto counties in Mississippi only contained one lightning strike. The Marshall County, Mississippi mini-supercell contained 13 total lightning strikes, 7 of those positive strikes and 6 of those negative. The slightly higher lightning production of this cell

resulted from a greater portion of the storm's core that remained above the freezing level for a slightly longer period of time.

4. RADAR INTERPRETATION

A large area of rain and thunderstorms were first detected by the KNQA radar (Millington, TN) moving into western portions of the Memphis County Warning Area (CWA) around 0800 UTC on 23 October 2004. This convection developed in advance of a pre-frontal trough that moved across Arkansas during the early morning prior to 1200 UTC. This convection remained elevated as it moved across portions of the CWA (east Arkansas, the Missouri Bootheel, west Tennessee, and north Mississippi). All of this convection remained below severe limits and greatly diminished in overall coverage by 1400 UTC. In the wake of this early morning convection, a mesohigh and associated cold pool remained over Arkansas. It was along the leading edge of this cold pool where Convective Outflow Boundary #1 (described above in the Pre-Storm Environment-Surface Conditions section) formed and moved east (Fig. 5).

By 1500 UTC, an area of increasing instability had developed southeast of Convective Outflow Boundary #1 and along an axis that stretched across the Mississippi River Delta to the south of Memphis. A new cluster of convection began to initiate within this instability axis as well as along Convective Outflow Boundary #1 as the 500 mb shortwave trough approached. This new convection continued to propagate northeast across portions of northwest Mississippi.

As the day progressed, a few of the thunderstorms from this new cluster became surface based, intensified, and became severe. There were several supercell thunderstorms that were of particular interest because of their diminutive sizes. Throughout the life cycle of these storms, storm tops remained low with average echo tops around 9.1 km (Davies, 1993) and significant storm echo diameters remained small (Kennedy et. al., 1993), as compared with typical Mid-South supercells. These miniature supercells were responsible for producing a series of funnel clouds, straight-line wind damage, and a tornado which produced F1 intensity damage as they progressed across north Mississippi.

The first thunderstorm of particular interest (named Storm A hereafter) was embedded within the new convective cluster that had developed over eastern Arkansas after 1500 UTC. As these thunderstorms moved across the Mississippi river into northwest Mississippi between 1530 UTC and 1709 UTC they organized into discrete cells. By 1709 UTC, Storm A crossed into northwest portions of Tunica County in northwest Mississippi and began to intensify as it interacted with Convective Outflow Boundary #1 (Fig. 14). This thunderstorm cell exhibited weak low- and mid-level storm rotation, storm echo tops ranging between 7.6 - 9.1 km, and a strengthening low level reflectivity gradient on the inflow side of the storm. In addition, stronger reflectivity echoes were noted with 50-55 dbz reflectivity extending to above 1.5 km.

By 1714 UTC, Storm A continued to become better organized with an improved reflectivity structure and increased low-level rotation as it moved northeast along Convective Outflow Boundary #1. This boundary extended across northwest Tunica County, Mississippi, into Shelby County, Tennessee. At this time, Storm A was located 79 km southwest of the KNQA radar site

and was moving northeast at 14 m s^{-1}. The storm updraft intensified between 1645 UTC and 1714 UTC with base reflectivity indicating 50-55 dbz echoes extending up to 3.6 km. Also, radar began to indicate the development of a more distinct echo overhang and the beginning of a low-level inflow notch (Fig. 15a). The low level rotation also began to strengthen by 1714 UTC with the mesocyclone extending from just above the surface to approximately 4.9 km. Rotational velocities ranged from 13 m s^{-1} at 1.0 km, to 6 m s^{-1} at 3.6 km. The strongest rotation was noted below 2.4 km and the mesocyclone first strengthened in the lowest levels, possibly indicative of a non-descending mesocyclone (Trapp et. al., 1999) (Fig. 15b). The storm had transitioned into a supercell thunderstorm by 1714 UTC but still remained quite small in size. Storm echo tops remained between 7.6 - 9.1 km, the 45 dbz storm echo diameter was measured at only 6 km, and the 25 dbz storm echo diameter was measured at 17 km (45 dbz and 25 dbz echo diameters are measured at the lowest elevation slice and hereafter refer to the low-level echo diameters).

Storm A strengthened further between 1714 UTC and 1749 UTC as it moved northeast out of Tunica county and across DeSoto county, Mississippi. Radar base reflectivity at 1749 UTC indicated a well developed echo overhang, a tighter inflow reflectivity gradient, and a more distinct low-level inflow notch (Fig. 16a). The mesocyclone continued to strengthen and became deeper with stronger rotation noted from 0.6 km above the ground to greater than 3.4 km. Rotational velocities ranged from 13 m s^{-1} at 0.7 km, to greater than 9 m s^{-1} at 3.3 km (Fig. 16b). In addition, the storm updraft intensified with 50-55 dbz echoes extending above 4.0 km and 55-60 dbz echoes noted at 1.6 km. The overall storm size still remained small at 1749 UTC with storm echo tops remaining below 9.1 km, the 45 dbz echo diameter at 11 km, and the 25 dbz echo diameter only 14 km. As the miniature supercell progressed across DeSoto County between 1732 UTC and 1807 UTC, several reports of a well developed wall cloud and funnel clouds were received from storm spotters in the area (Fig. 17).

By 1807 UTC, the miniature supercell attained maximum intensity 43 km south of the KNQA radar site as it traversed just north of Convective Outflow Boundary #1. By this time, the boundary stretched across DeSoto County, Mississippi. The mesocyclone continued to strengthen at the lowest elevation slice with rotational velocity in excess of 18 m s^{-1} (Fig. 18a). However, the magnitude of rotational velocity slightly decreased from 9.1 m s^{-1} to 8 m s^{-1} at 2.4 km between 1749 UTC and 1807 UTC. The updraft strength also continued to improve with a 50-55 dbz core extending to 3.0 km with 55-60 dbz reflectivity noted at 2.5 km. The storm's echo overhang was still quite pronounced at 1807 UTC while a low-level inflow notch was persistent along the southeast flank of the mini-supercell (Fig. 18b). One important feature to note was the continued small size of the storm even at maximum intensity. Storm echo tops remained between 7.6 - 9.1 km, the 45 dbz echo diameter was measured at 13 km, and the 25 dbz echo diameter was 19 km. Storm spotters were still reporting funnel clouds in association with the storm at this time.

The mini-supercell thunderstorm (Storm A) significantly weakened after 1807 UTC as it continued to move northeast at 14 m s^{-1}. By 1813 UTC, there was a significant degradation of the mesocyclone as the storm moved several kilometers north of Convective Outflow Boundary #1 and into a more stable airmass. Beyond 1813 UTC, the low-level rotation and high reflectivity core had dissipated bringing an end to the severe weather threat associated with this storm.

Additional thunderstorms developed through 1900 UTC further southwest from where Storm A originated. This development occurred along Convective Outflow Boundary #1. One of these storms (named Storm B hereafter) was of particular interest. Storm B developed around 1700 UTC to the west of the Mississippi River and propagated east along Convective Outflow Boundary #1 into northwest Mississippi by 1807 UTC. Storm B remained below severe limits through 1830 UTC as it exhibited weak to moderate reflectivities and weak low-level storm rotation. Between 1830 UTC and 1842 UTC, Storm B merged along the trailing side of a new convective cell (named Storm C hereafter) moving northeast. Storm C was one of several discreet convective elements that developed in the increasingly unstable airmass to the southeast of Convective Outflow Boundary #1 and downwind from Storm B. Outflow associated with these newly formed convective elements created Convective Outflow Boundary #2 which moved northward. As Storm B interacted with Storm C and Convective Outflow Boundary #2 between 1836 UTC and 1842 UTC, Storm B rapidly weakened. The rapid weakening of Storm B likely resulted from Storm C inhibiting the supply of warm-moist inflow air into Storm B's updraft region. These findings concur with the investigations of Przybylinski and Wright (1986) and Wolf et al. (1996). However, this type of storm evolution and merger is in contrast to observations documented by Klemp et. al. (1980) in which outflow from developing storms upwind disrupts inflow into stronger downwind storms resulting in rapid deterioration of the downwind storms. Also during this time period, Convective Outflow Boundary #2 merged with Convective Outflow Boundary #1(hereafter the merged boundary will be referred to as Convective Outflow Boundary #3) and provided a favorable environment for Storm C to intensify.

By 1905 UTC, Storm C had rapidly intensified while propagating along Convective Outflow Boundary #3 over southeastern Tunica County. Radar reflectivity signatures improved with a strong low-level reflectivity gradient evident along the inflow side of the storm (Fig. 19a). The storm updraft also became better established with maximum reflectivity values of 50-55 dbz extending from near the surface to 4.3 km. Low-level storm rotation increased as well with rotational velocities of 13 m s^{-1} noted at 1.3 km (Fig. 19b). Much weaker and broader rotation was detected at 2.7 km with the rotation becoming indiscernible at higher altitudes. The mesocyclone associated with Storm C first developed in the low-levels as was seen with Storm A and can be classified as nondescending (Trapp et. al., 1999). It is believed that Convective Outflow Boundary #3 played an important role in enhancing low-level vorticity (Moller et. al., 1990) (Rasmussen and Blanchard, 1998). It is hypothesized that this increased low-level vorticity, once ingested into Storm C, strengthened the low-level mesocyclone. In addition, inflow into the updraft of Storm C remained warm, moist, and convectively undisturbed. This moisture rich air combined with the increased low-level vorticity to produce rapid intensification of Storm C between 1842 UTC and 1905 UTC. Storm C still remained small in overall size (although larger than Storm A) with storm echo tops ranging between 9.1 km and 10.7 km, the 45 dbz echo diameter measured at 17 km, and the 25 dbz echo diameter measured at 24 km.

Between 1905 UTC and 1916 UTC, the initial mesocyclone associated with Storm C occluded into the rain-cooled air. A new mesocylone developed along the rear flank downdraft located on the southern flank of Storm C (Fig. 20). This thunderstorm remained nearly steady-state between 1916 UTC and 1951 UTC as the storm moved east from eastern Tunica county into Tate county. Storm C continued to propagate eastward at 11 m s^{-1} along Convective Outflow Boundary #3. The

low-level rotation remained steady but shallow, with the strongest rotation remaining below 2.1 km. Rotational velocities at 1951 UTC ranged from 13 m s^{-1} at 1.1 km to 5 m s^{-1} at 2.4 km. Reflectivity values at 1951 UTC actually decreased with maximum reflectivity values of 50-55 dbz extending up to 3.4 km, as compared to similar reflectivity values up to 4.3 km at 1905 UTC. Storm echo tops dropped to between 7.6 - 9.1 km, but the low level echo diameter increased. The 45 dbz echo diameter extended to 24 km and the 25 dbz echo diameter stretched to 34 km. The overall appearance of the storm at 1951 UTC was characterized by a lower echo top and a larger storm diameter.

By 2009 UTC, Storm C began a second intensification cycle across eastern Tate county with rapid intensification of a second mesocyclone, especially in the lowest levels. Rotational velocities increased to 20 m s^{-1} at 1.0 km, 15 m s^{-1} at 2.3 km, and 13 m s^{-1} at 3.4 km (Fig. 21a). The mesocyclone had deepened resulting in higher rotational velocity magnitudes throughout the entire depth of the mesovortex. In addition, reflectivity values once again increased with 50-55 dbz values detected up to near 4.6 km. The overall reflectivity structure of Storm C intensified with the development of a recognizable inflow notch, a strong low-level reflectivity gradient evident along the storm's southern flank, and a better developed echo overhang (Fig. 21b). An appendage also appeared on the inflow side of the storm and is believed to be the development of a flanking line. The overall size of the storm decreased as the storm intensity increased between 1951 UTC and 2009 UTC. Storm echo tops ranged between 7.6 - 9.1 km, the 45 dbz echo diameter retracted back to 17 km, and the 25 dbz echo diameter retracted back to 25 km.

Several important structural changes were noted with Storm C as it moved from eastern Tate county into Marshall county between 2009 UTC and 2038 UTC. During this time period, the reflectivity core began to collapse with 50-55 dbz reflectivity values dropping from around 4.6 km at 2009 UTC to below 3.4 km at 2038 UTC. In addition, reflectivity values at 7.6 km decreased from 30-35 dbz at 2009 UTC to 15-20 dbz at 2038 UTC. The reflectivity features also became degraded at 2038 UTC with the once distinct inflow notch indiscernible and the echo overhang no longer detected (Fig. 22a). As the reflectivity structure collapsed, the low-level rotational velocities rapidly increased in magnitude. At 2038 UTC, rotational velocities were maximized and ranged from 23 m s^{-1} at 1.0 km to 8 m s^{-1} at 3.3 km (Fig. 22b). These observations of storm collapse and increase in low-level rotation are similar to observations noted by Burgess et al. (1982) in their study of tornadic supercell thunderstorms across Oklahoma. This increase in maximum rotational velocities and decrease in height of the maximum rotational velocities prior to the time of tornadogenesis also correlates well with the findings of Grant and Prentice (1996) in their study of mini-supercell thunderstorm characteristics. One deviation from the findings of Grant and Prentice (1996) concerned the maximum strength of the low-level mesocyclone. Grant and Prentice (1996) found that the average values of maximum rotational velocities and lowest level velocities fell into the "minimal"category on the Operational Support Facilities (OSF) - Mesocyclone Strength Nomogram (MSN). In this case, Storm C acquired maximum rotational velocities that fell into the "strong" category on the OSF - MSN. Therefore, although many miniature supercell thunderstorms only produce weak mesocyclones, it is still possible for these type of thunderstorms to produce strong mesocyclones at low-levels. It was at 2038 UTC that Storm C moved into the community of Marianna in Marshall county and spawned a tornado that resulted in F1 intensity damage to structures and trees (Fig. 23).

As Storm C moved further east it transitioned into a bow echo and produced additional areas of straight-line wind damage across northern portions of Mississippi. There were no additional reports of structural damage to the east of Marshall County.

5. DISCUSSION AND SUMMARY

There are important considerations to keep in mind during convective events that were learned during this case study. These considerations will have important implications on both convective initiation and intensification and the warning decision process. It remains important to be cognizant of pre-existing low-level boundaries that may aid convective development and intensification. In addition, it is important to remain aware of existing or changing local environments that will determine convective mode during events.

Pre-existing low-level boundaries are important during active convective events because they can influence storm initiation and intensification. On 23 October 2004 three notable convective outflow boundaries are believed to have played an important role in locally enhancing low-level vorticity and impacting storm intensity (Markowski et al., 1998). With respect to Storm A, low-level vorticity was believed to be enhanced as it became rooted and moved east along Convective Outflow Boundary #1. This was evident by the reports of well developed wall clouds and funnel clouds. As Storm B developed and moved along Convective Outflow Boundary #1, it interacted with Convective Outflow Boundary #2. Convective Outflow Boundary #2 was generated by warm sector convection and this became important to the eventual demise of Storm B and rapid evolution of a new thunderstorm (Storm C). Storm C became rooted along a newly merged convective boundary (Convective Outflow Boundary #3) and ingests enhanced low-level vorticity generated along the boundary. This appears to correlate well with the findings from VORTEX-95 (Markowski et al., 1998). Storm C eventually produced tornado that resulted in F1 damage following the boundary interaction, mesocyclone occlusion, and storm collapse. So it is important to remain aware of convective boundaries and their interactions, as they are believed to impact storm evolution, enhance low-level vorticity, and possibly enhance tornadogenesis potential.

Understanding the local environment prior to and during convective events also remains important. When local environments exhibit limited instability and moderate to high levels of environmental shear, low-topped supercell thunderstorms become the expected convective mode. Distribution of existing CAPE through the atmosphere also appears important. Miniature supercells seem to favor larger amounts of CAPE in the lowest levels of the environment, with limited instability in the upper levels of the atmosphere. This helps to keep storm tops low because the convection that develops in this type of an environment can only realize the larger CAPE in the lower levels.

Once a favorable environment for miniature supercells is in place and this type of convection develops, it becomes vital that warning meteorologists recognize the threats associated with these storms. It is important for the warning meteorologist to assess the existing environment, anticipate the mode of convection most likely to develop, and remain cognizant of changing environments that may allow the convective mode to change. Well established conceptual models can also strengthen the warning meteorologists arsenal for decision making during the warning

process.

In order to better prepare meteorologists for miniature supercell events in the future, additional training should be provided. Additional research and case studies concerning these events can also help to improve understanding and detection. With continued training and experience, severe weather warnings during low-topped convective events will improve.

6. ACKNOWLEDGMENTS

The authors would like to dedicate this research to the life of Dr. Roderick Scofield. His enthusiasm and love for the field of meteorology and research along with his personal encouragement and editing have made this manuscript possible.

The authors would also like to express great gratitude to Ron Pryzbylinski for his insightful personal communications and scientific review of this manuscript. Thanks also to Scott J. McNeil and Scott C. Cordero for their assistance with data analysis. Additional thanks goes to Anthony Cavallucci for his assistance with web conversion and graphics production.

7. REFERENCES

Bluestein, H.B., 1993: Synoptic-Dynamic meteorology in mid-latitudes. Volume II. Oxford Univ. Press, pp. 398-399.

Burgess, D.W., R.R. Lee, S.S. Parker, and D.L. Floyd, 1995: A study of mini supercells observed by WSR-88D radars. Preprints 27th Conf. On Radar Meteorology, Vail, CO, Amer. Meteor. Soc.

____, V.T. Wood, and R.A. Brown, 1982: Mesocyclone evolution statistics. 12th Conf. On Severe Local Storms, San Antonio, TX, Amer. Meteor. Soc., pp. 422-424.

Davies, J.M., 1993: Small tornadic supercells in the southern plains. Preprints 17th Conf. On Severe Local Storms and Atmospheric Electricity, St. Louis, MO, Amer. Meteor. Soc.

Gerard, A.E., G.R. Garrett, and C. Morgan, 2000: An overview of a cool season tornadic supercell over central Mississippi. Nat. Wea. Assoc. Electronic Journal, 2000-EJ2.

Grant, B., and R. Prentice, 1996: Mesocyclone characteristics of mini supercell thunderstorms. Preprints 15th Conf. on Weather Analysis and Forecasting. Norfolk, VA, Amer. Meteor. Soc., pp. 362-365.

Kennedy, P.C., N.E. Westcott, and R.W. Scott, 1993: Single doppler radar observations of a mini-supercell tornadic thunderstorm. Mon. Wea. Rev., Vol. 121, No. 6, pp. 1860-1870.

Klemp, J.B., P.S. Ray, and R.B. Wilhelmson, 1980: Analysis of merging storms on 20 May 1977. Preprints 19th Conf. on Radar Meteorology. Boston, MA, Amer. Meteor. Soc., pp. 317-324.

Markowski, P.M., E.N. Rasmussen, and J.M. Straka, 1998: The occurrence of tornadoes in supercells interacting with boundaries during VORTEX-95. Wea. Forecasting, Vol. 13, No. 3, Part 2, pp. 852-859.

____, J.M. Straka, 2000: Some observations of rotating updrafts in a low-buoyancy, highly sheared environment. Mon. Wea. Rev., Vol. 128, No. 2, pp. 449-461.

Moller, A.R., C.A. Doswell, and R. Przybylinski, 1990: High-Precipitation Supercells: A conceptual model and documentation. Preprints, 16th Conf. On Severe Local Storms, Alberta, Canada, Amer. Meteor. Soc.

Przybylinski, R.W., and J.E. Wright, Jr., 1986: Analysis of severe convection and merging storms on 22 June 1984 with conventional and dopplar radar. Nat. Wea. Digest, Vol. II, No. 3, pp. 6-17.

Rasmussen, E.N., and D.O. Blanchard, 1998: A baseline climatology of sounding-derived supercell and tornado forecast parameters. Wea. Forecasting, Vol. 13, pp. 1148-1164.

Trapp, R.J., E.D. Mitchell, G.A. Tipton, D.W. Effertz, A.I. Watson, D.L. Andra Jr., and M.A. Magsig, 1999: Descending and nondescending tornadic vortex signatures detected by WSR-88Ds. Wea. Forecasting, Vol. 14, No. 5, pp. 625-639.

Wicker, L.J., and L. Cantrell, 1996: The role of vertical buoyancy distributions in miniature supercells. Preprints, 18th Conf. On Severe Local Storms, San Francisco, CA, Amer. Meteor. Soc.

Wolf, R.A., R.W. Przybylinski, and P. Berg, 1996: Observations of a Merging Bowing Segment and Supercell. Preprints, 18th Conf. on Severe Local Storms, San Francisco, CA, Amer. Meteor. Soc. 740-745.

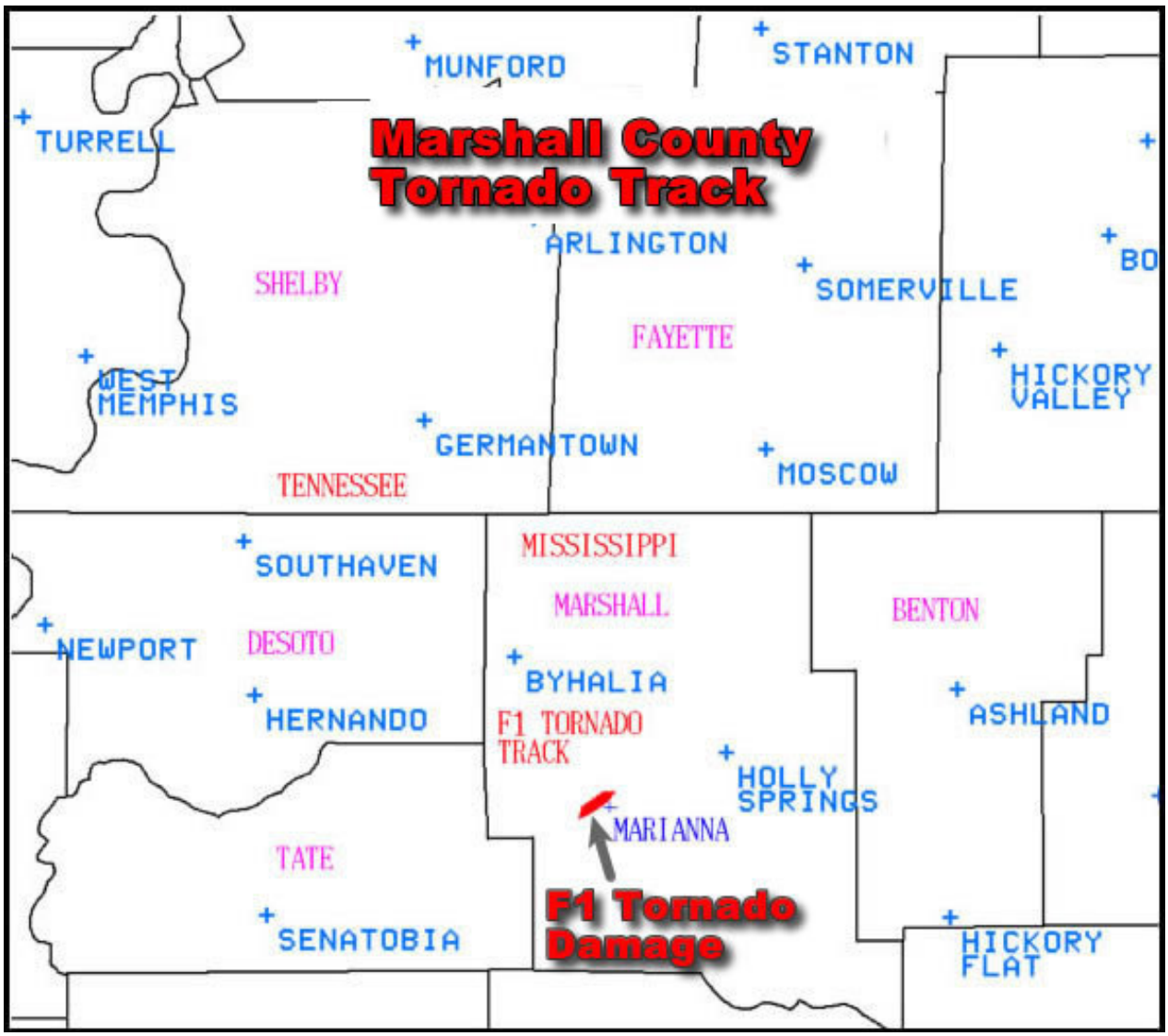

Figure 1. Track of F1 Marshall County Tornado (Red). All of the damage associated with the tornado occurred in Marianna, Mississippi.

Figure 2. Significant roof damage resulting from the Marshall County tornado.

Figure 3. Several large trees downed by the F1 intensity tornado.

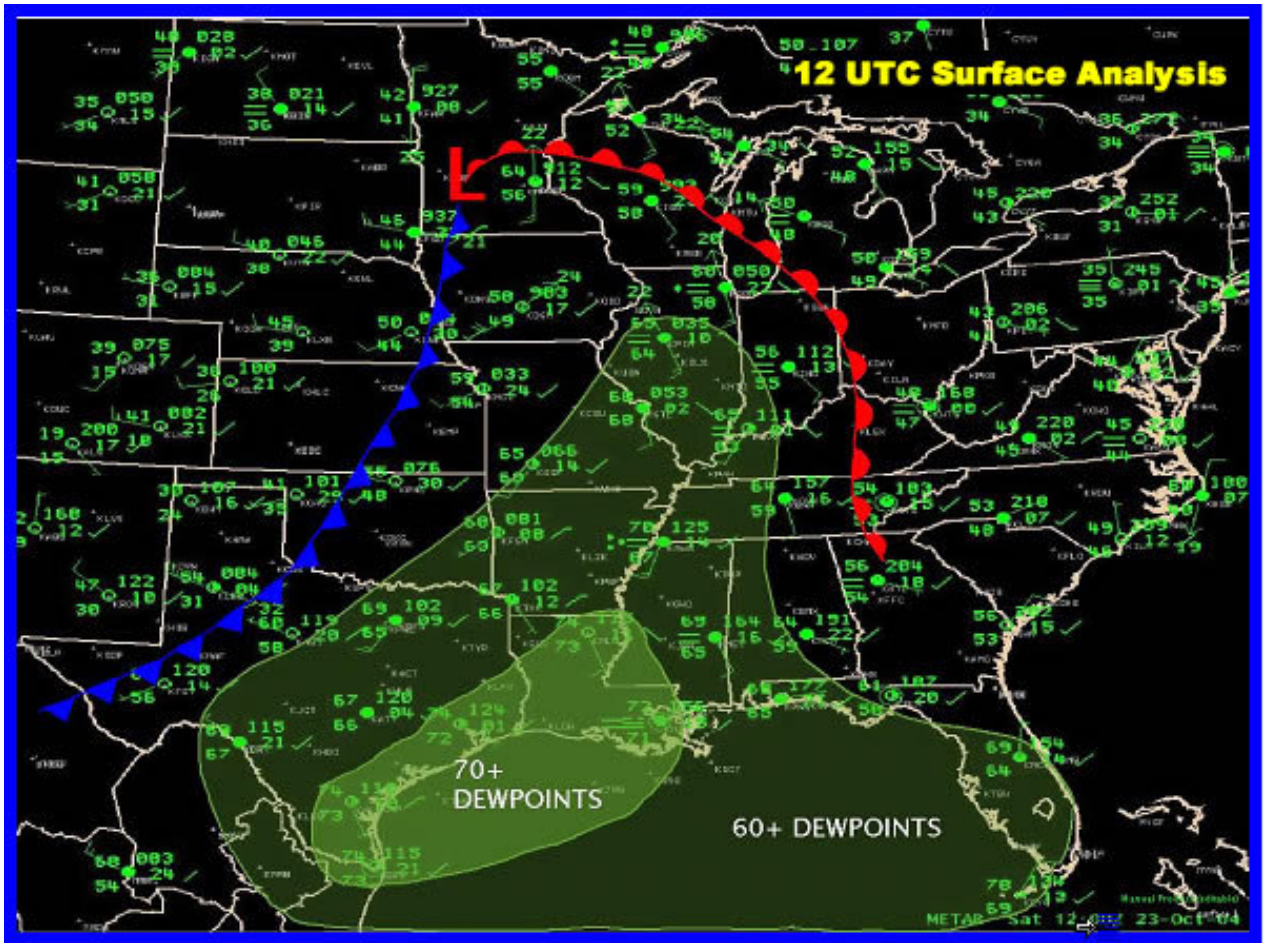

Figure 4. Surface Analysis from 1200 UTC, 23 October 2004. Frontal boundary positions are marked by standard surface boundary symbols. Dewpoint temperatures are shaded in green with the darker shaded areas indicative of higher surface dewpoint temperatures.

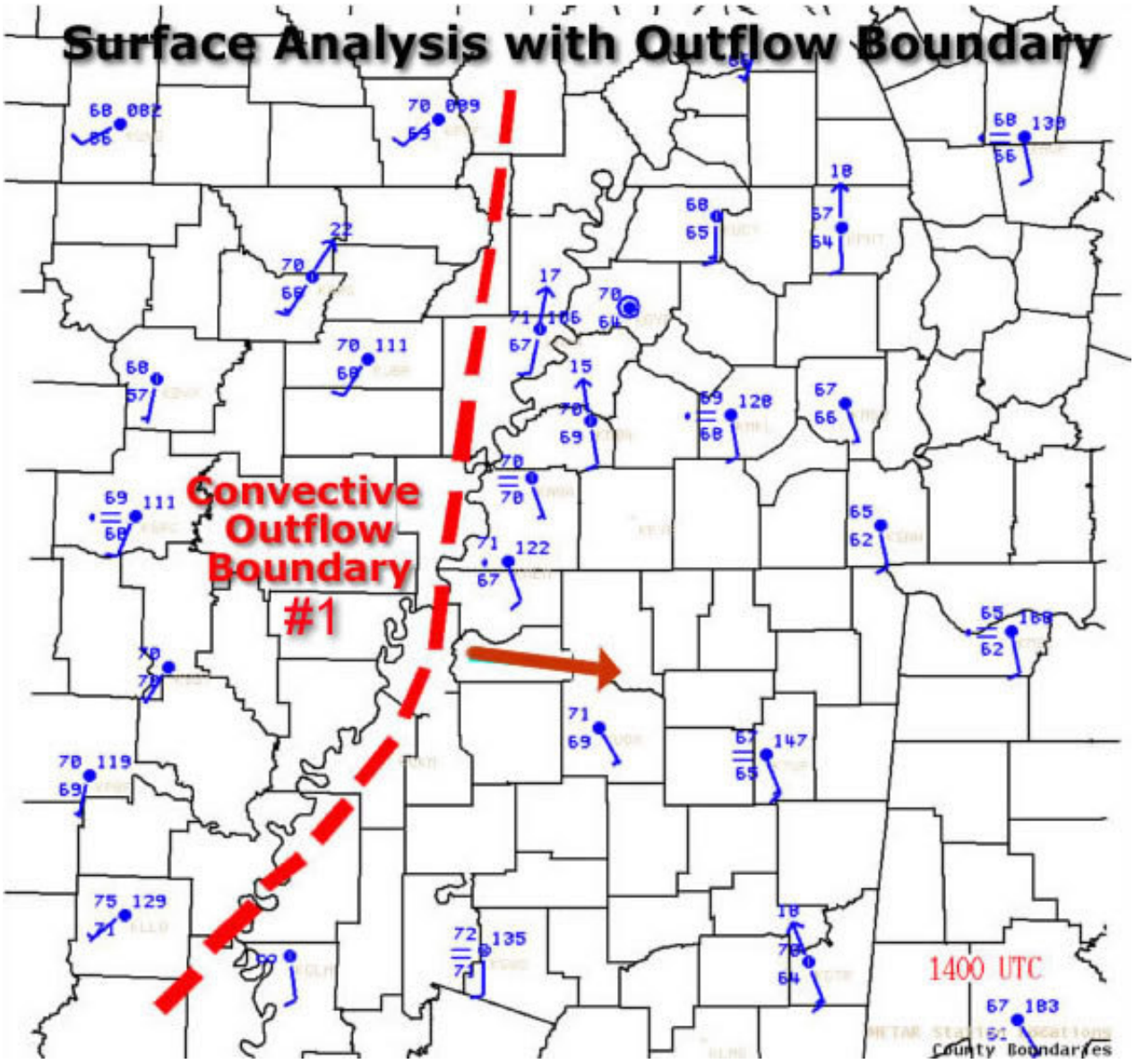

Figure 5. Surface Analysis from 1400 UTC, 23 October 2004. Convective Outflow Boundary #1 was stretched along the Mississippi River and moved east through the day. This boundary served as a focusing mechanism for convective development and a source for enhanced low level vorticity.

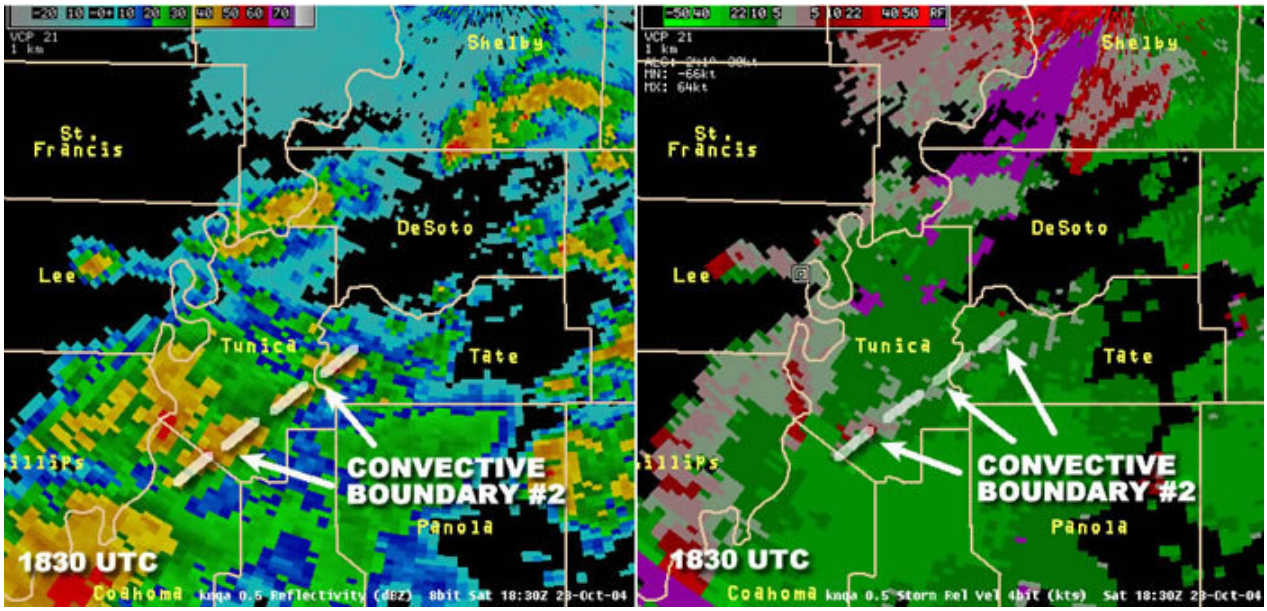

Figure 6. Surface Analysis from 1830 UTC, 23 October 2004. Convective Outflow Boundary #2 was formed from the outflow of developing convection over the warm sector. This boundary was instrumental in influencing convective development.

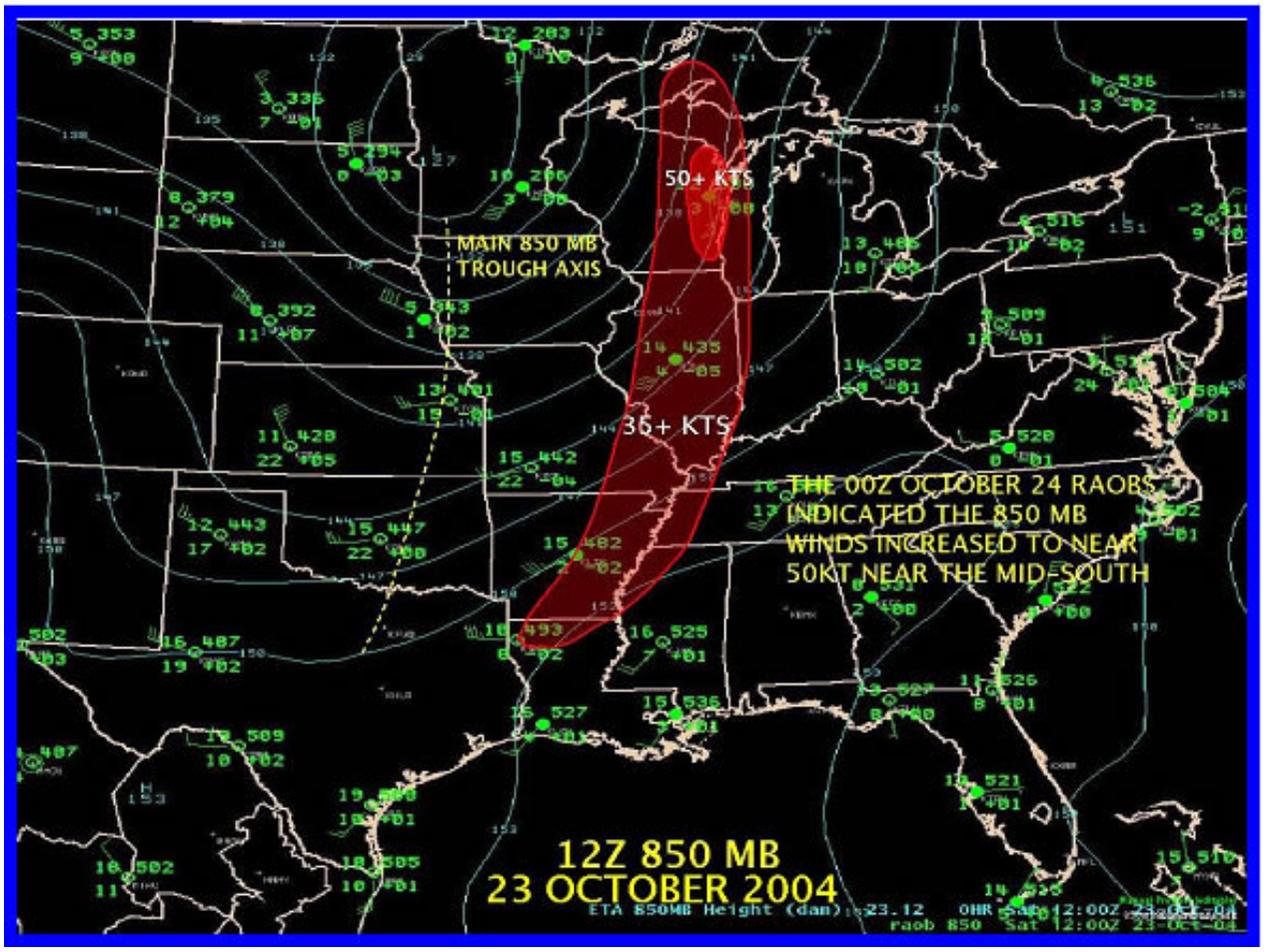

Figure 7. 850 MB Analysis from 1200 UTC, 23 October 23 2004. The red colored areas indicate the location of enhanced 850 mb wind speeds. The 850 mb trough axis is denoted by the dashed yellow line and was analyzed using the 850 mb raobs.

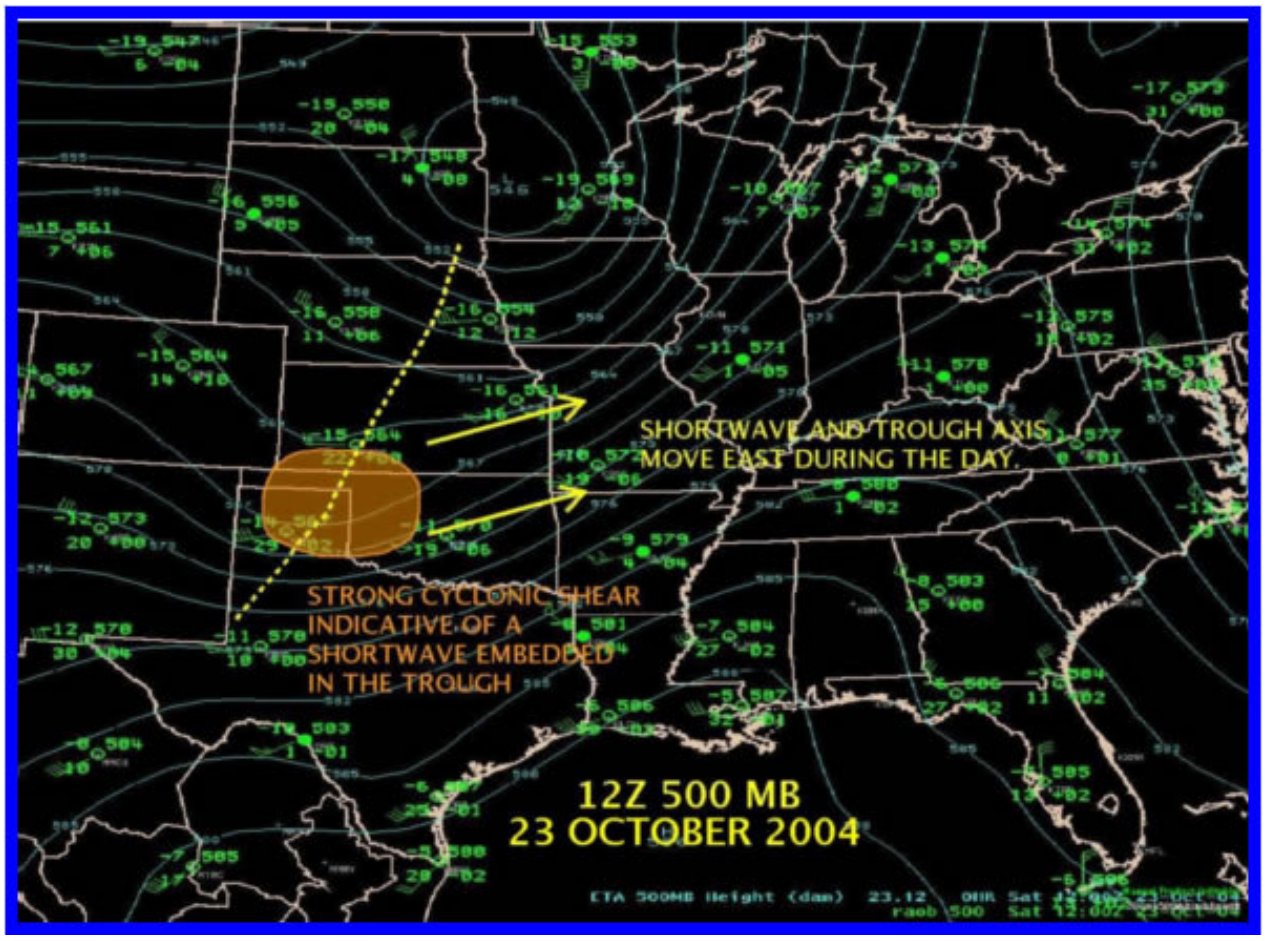

Figure 8. 500 MB Analysis from 1200 UTC, 23 October 2004. The orange colored area indicates the location of strong cyclonic shear. The 500 mb trough axis is denoted by the dashed yellow line and was analyzed using the 500 mb raobs.

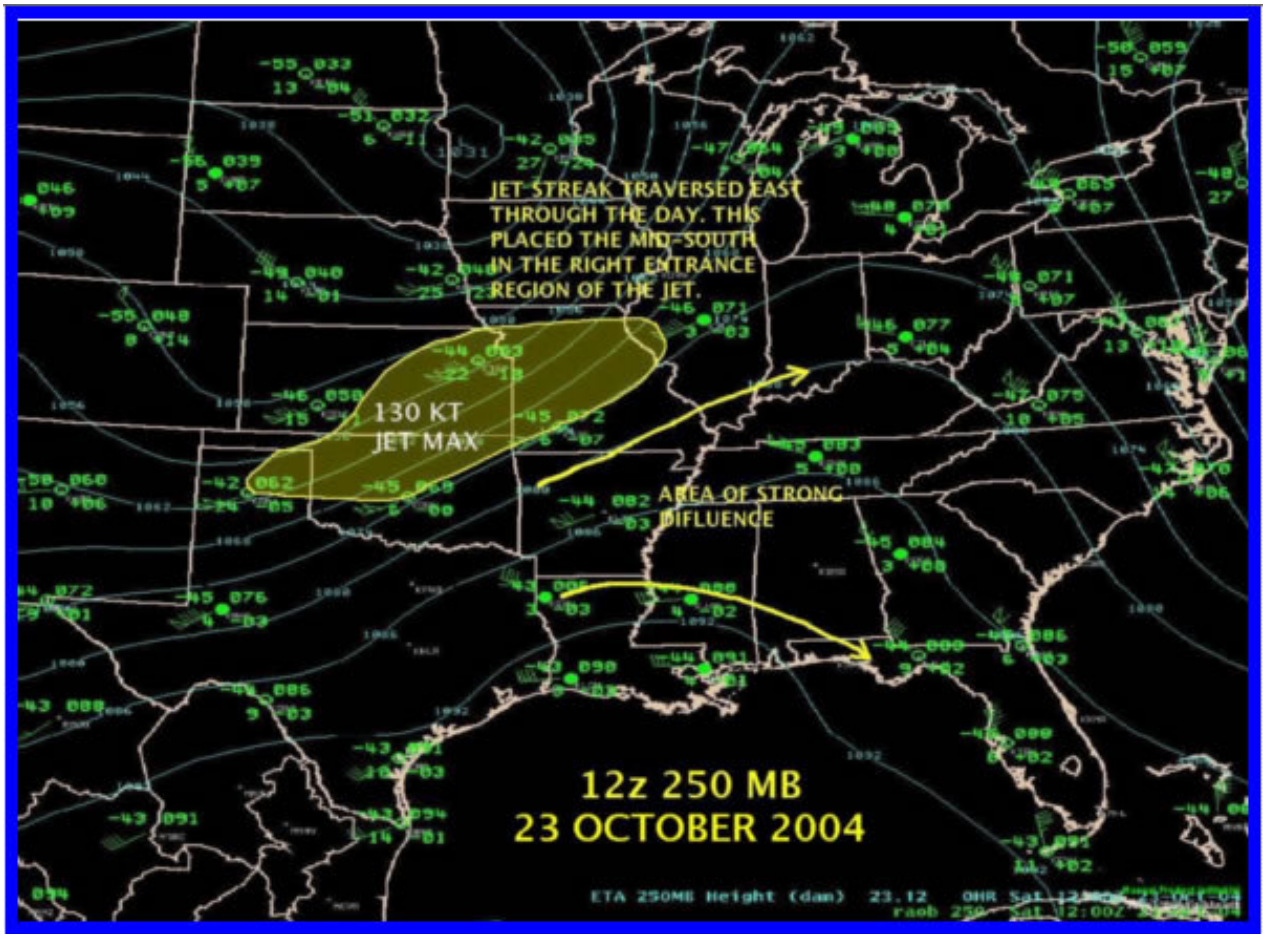

Figure 9. 250 MB Analysis from 1200 UTC, 23 October 2004. The yellow colored area indicates the location of a 130 kt upper-level jet maximum. An area of enhanced upper level difluence was noted in the right entrance region of the jet maximum and was analyzed using the 250 mb raobs.

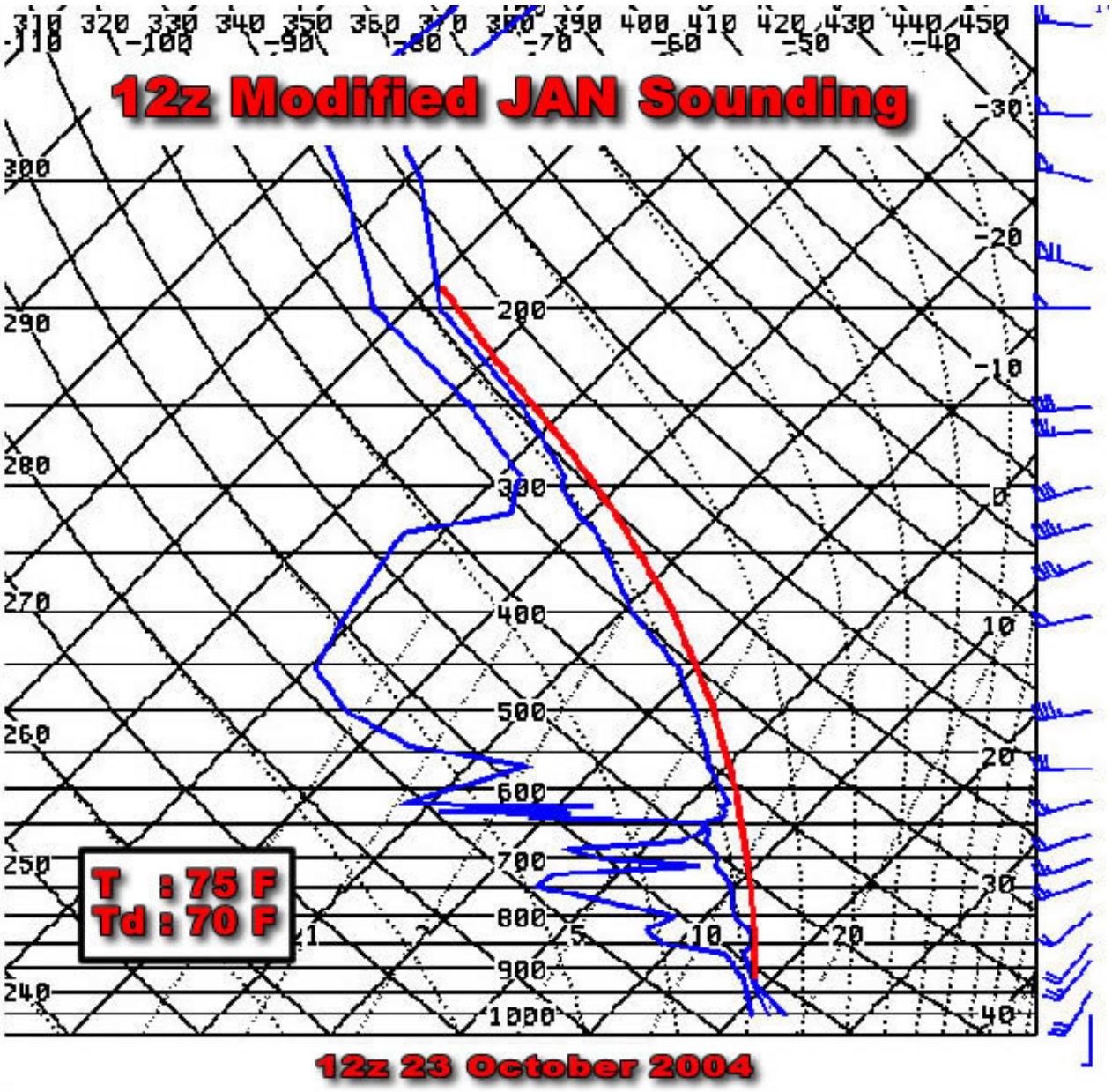

Figure 10. 1200 UTC, 23 October 2004, Jackson, Mississippi sounding modified for afternoon surface parcel using surface observations measured in proximity to the location and time of tornadogenesis.

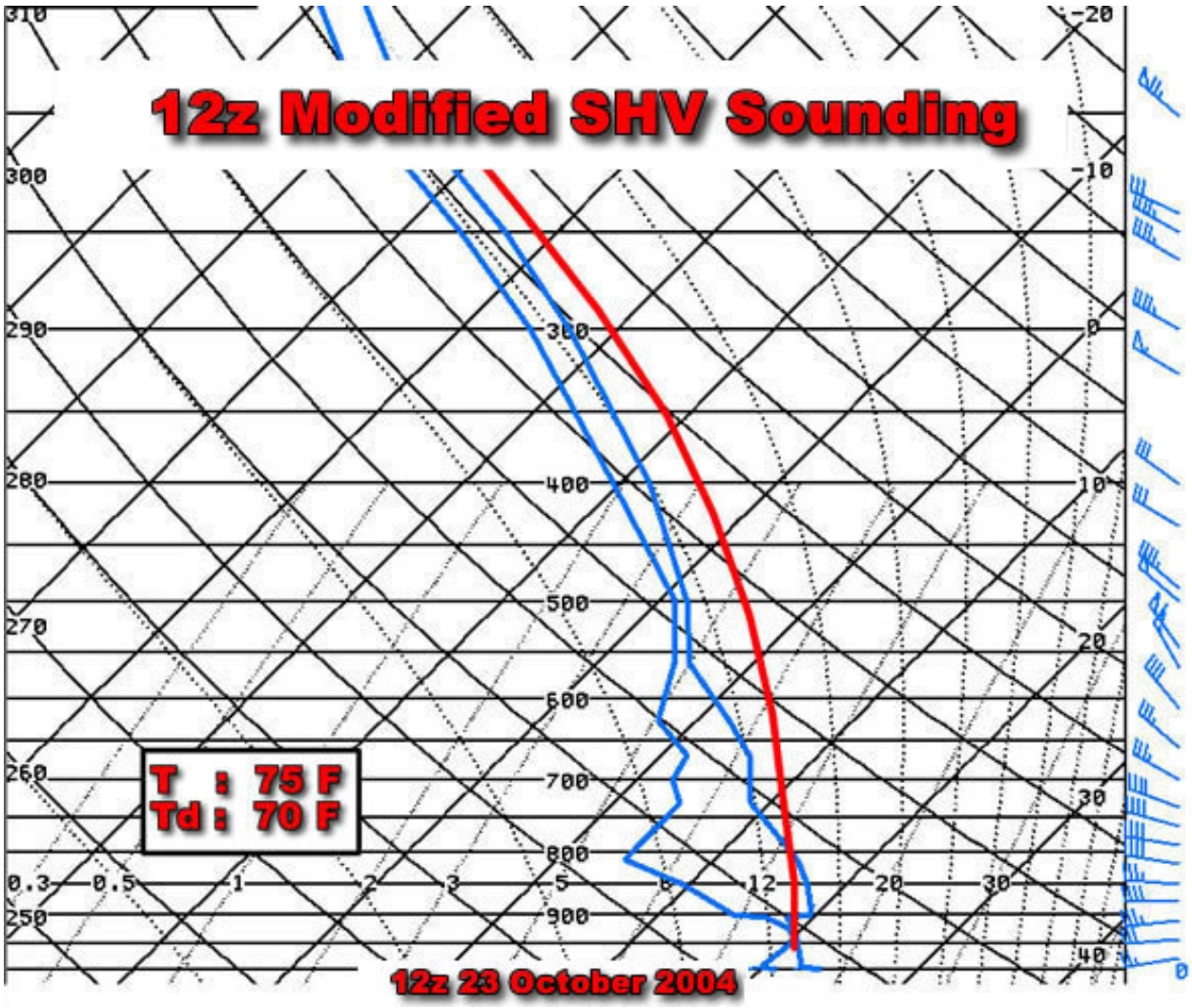

Figure 11. 1200 UTC, 23 October 2004, Shreveport, Louisiana sounding modified for afternoon surface parcel using surface observations measured in proximity to the location and time of tornadogenesis.

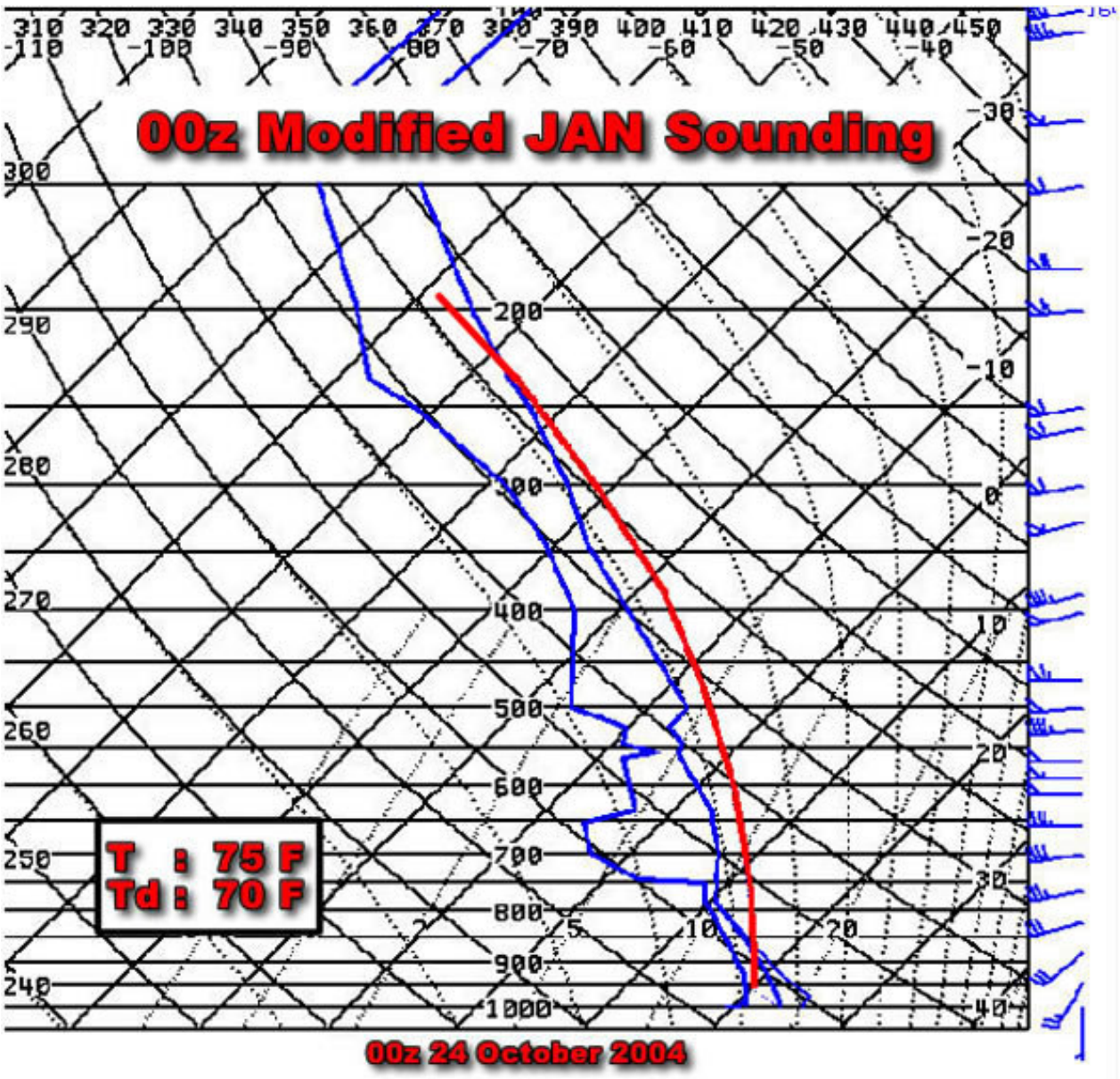

Figure 12. 0000 UTC, 24 October 2004, Jackson, Mississippi sounding modified for afternoon surface parcel using surface observations measured in proximity to the location and time of tornadogenesis.

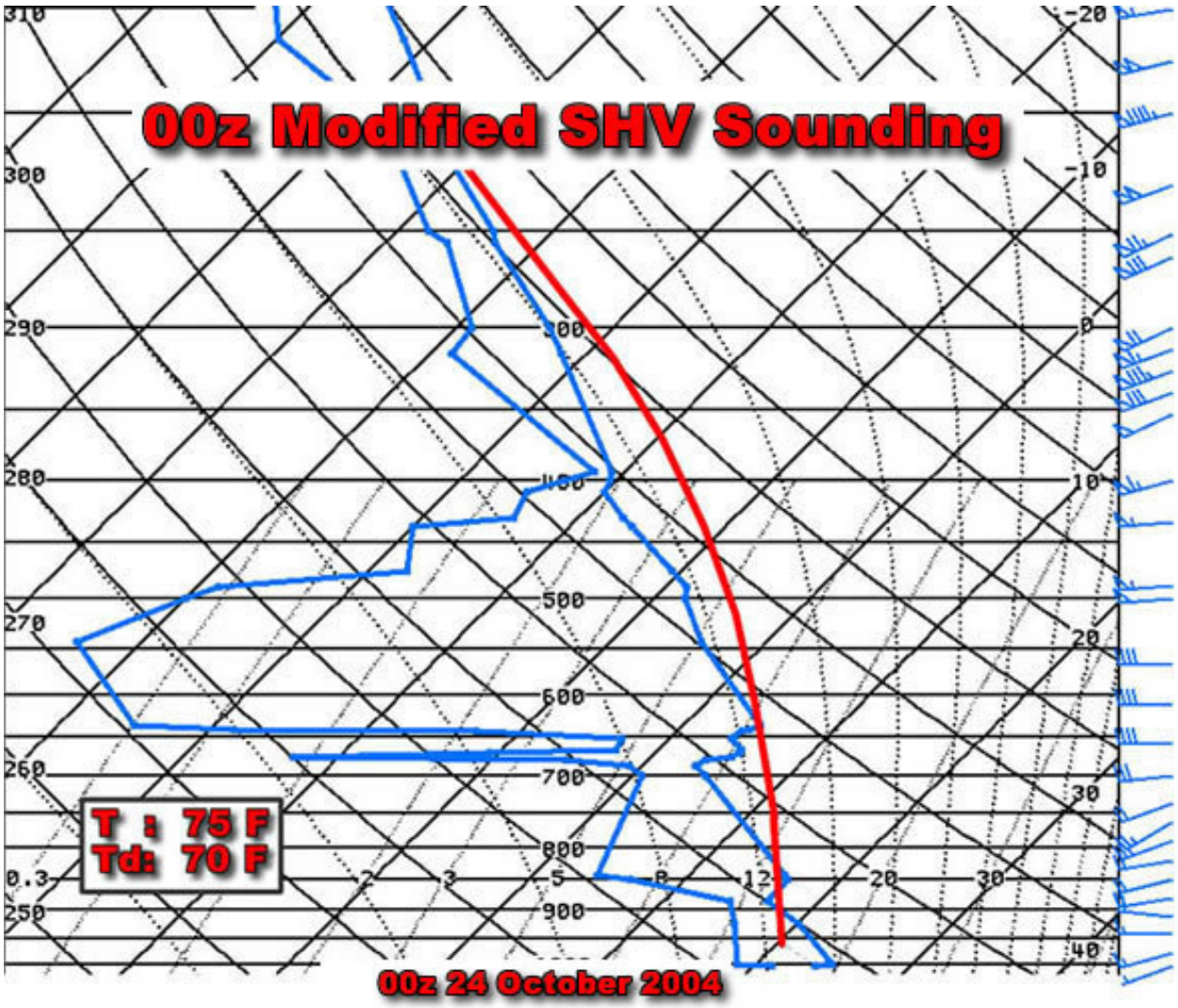

Figure 13. 0000 UTC, 24 October 2004, Shreveport, Louisiana sounding modified for afternoon surface parcel using surface observations measured in proximity to the location and time of tornadogenesis.

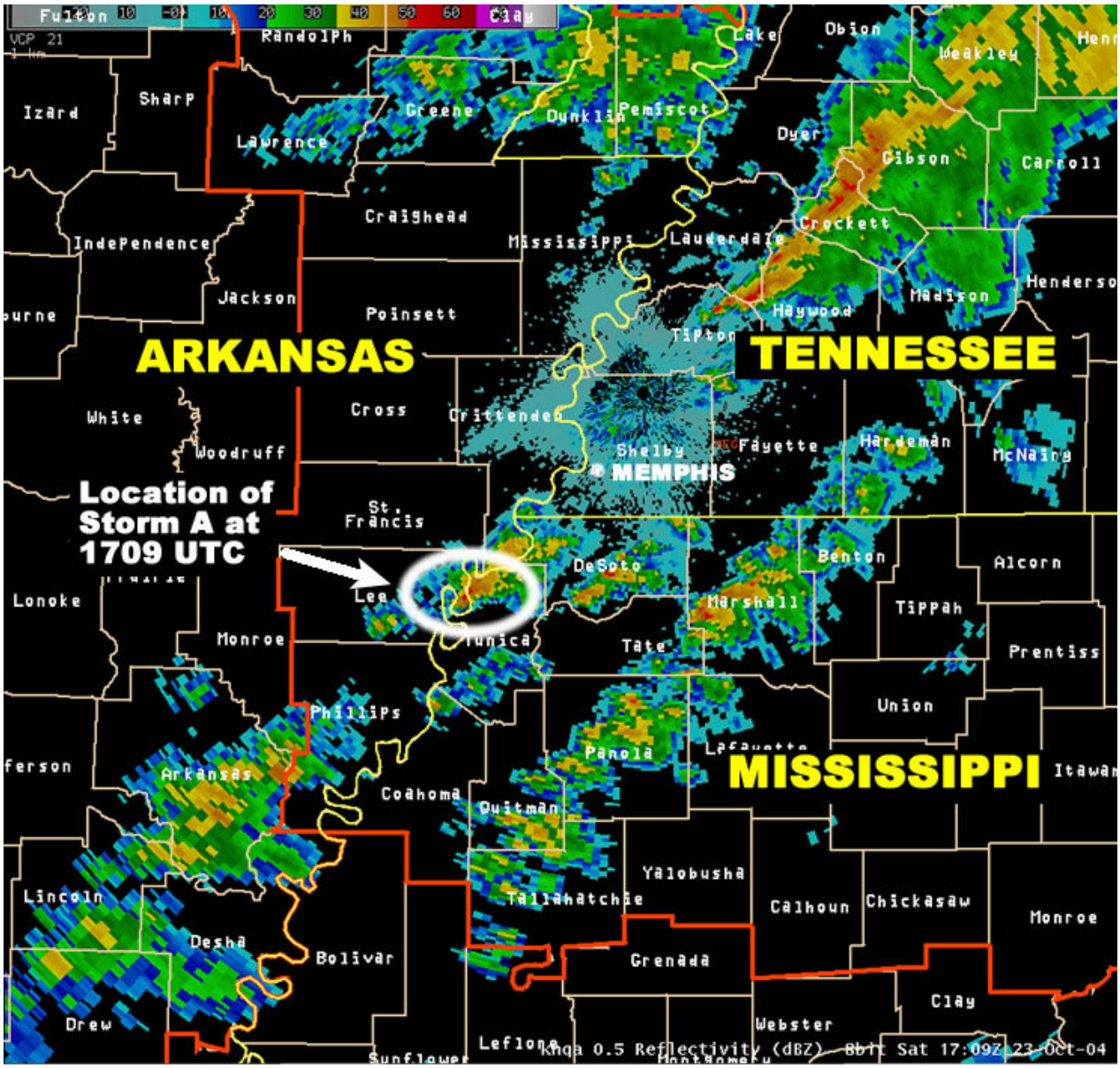

Figure 14. Location of Storm A as it moved into northwest Mississippi and strengthened.

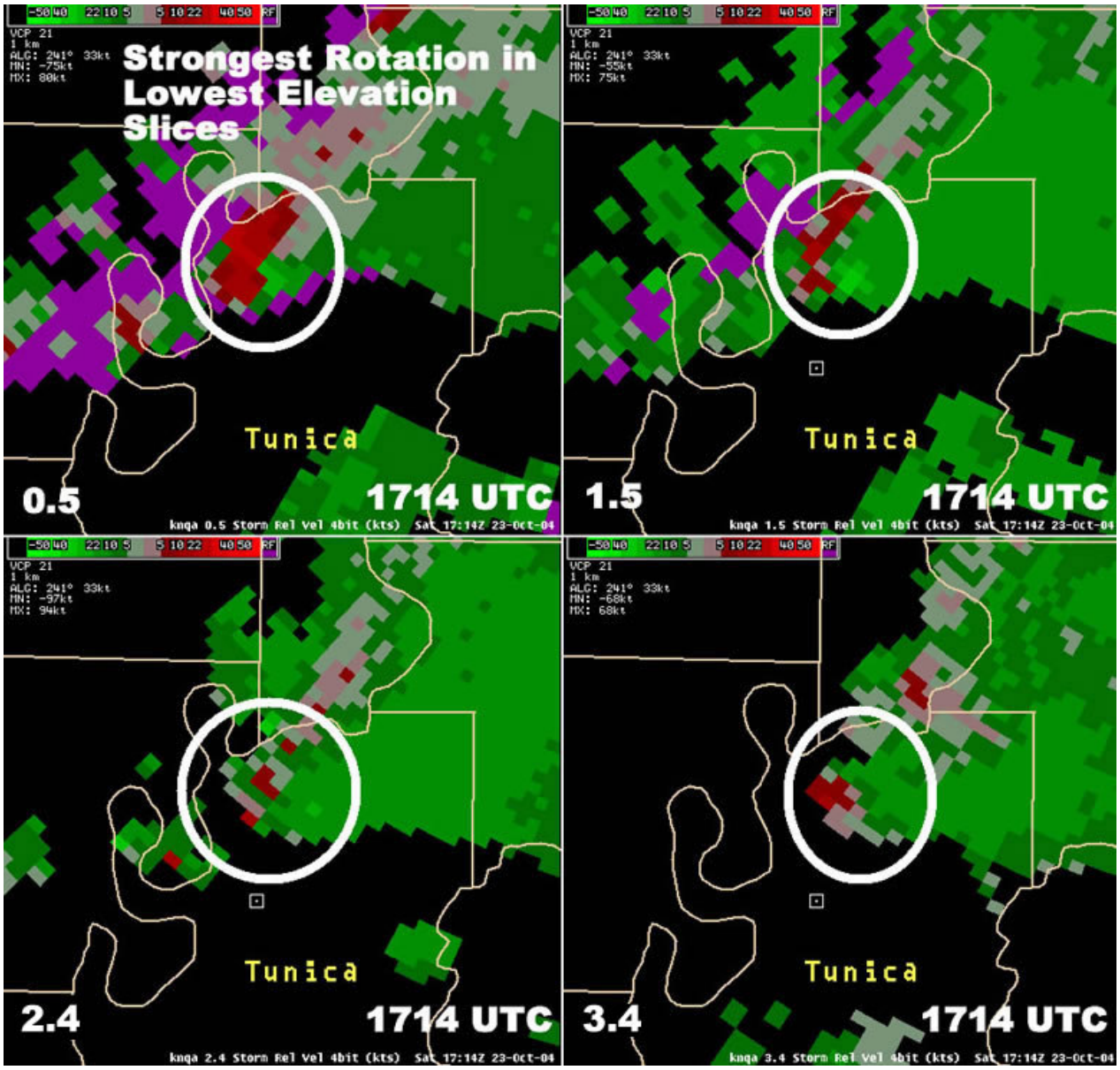

Figure 15a. Four panel display of Storm Relative Mean Velocity (SRM) at 1714 UTC, 23 October 2004. This SRM four panel display shows that the strongest rotation first developed in the lowest elevation slices, which is indicative of a nondescending mesocyclone.

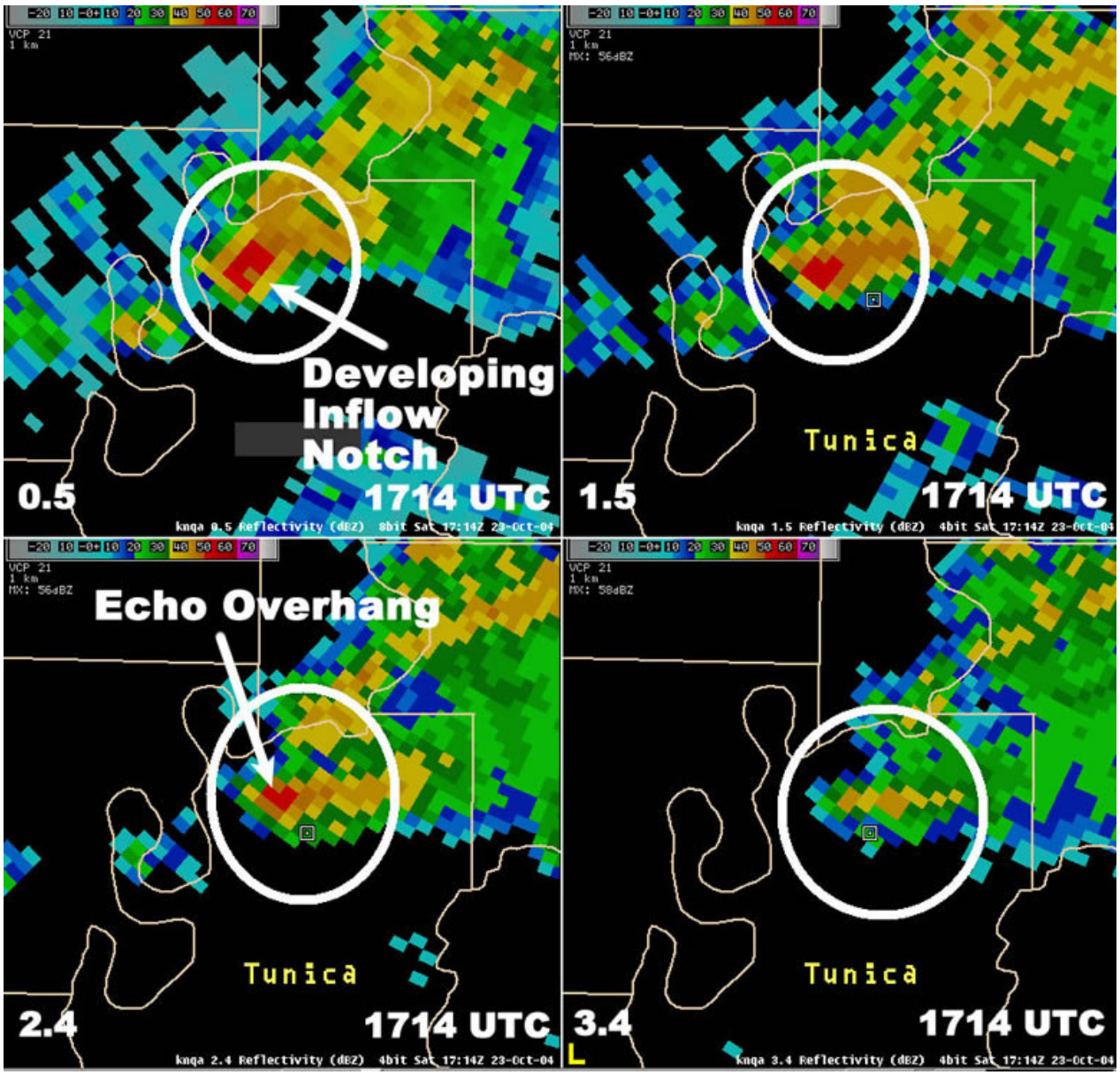

Figure 15b. Four panel display of Base Reflectivity (BREF) at 1714 UTC, 23 October 2004. This BREF four panel display shows improvement in the overall reflectivity structure of the storm with a developing low level inflow notch, a tight reflectivity gradient on the inflow side of the storm, and the presence of an echo overhang.

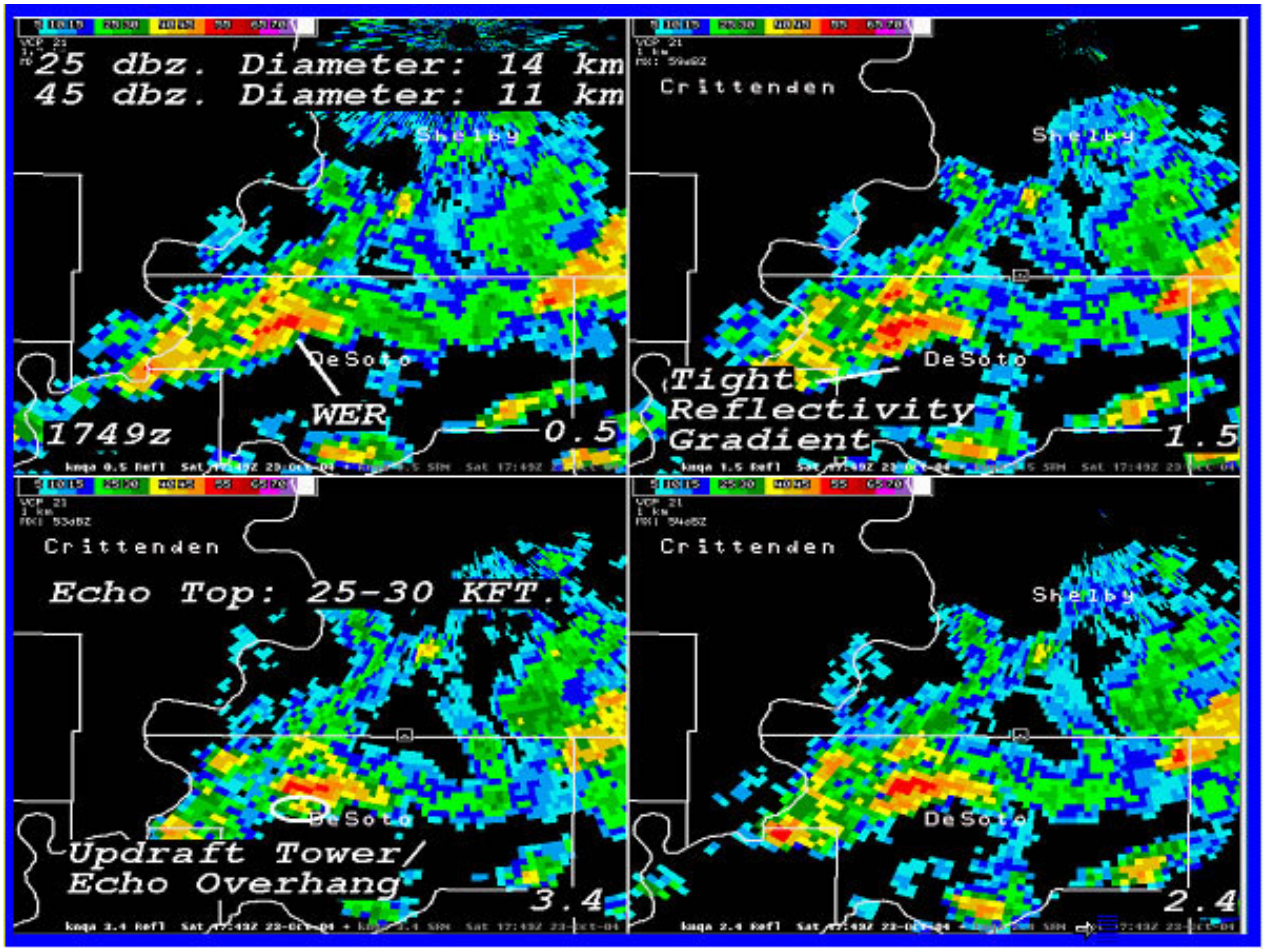

Figure 16a. The four panel display of Base Reflectivity (BREF) at 1749 UTC, 23 October 2004 indicated a small storm diameter with continued tight reflectivity gradient on the inflow side of the storm, a weak echo region, and a better developed echo overhang.

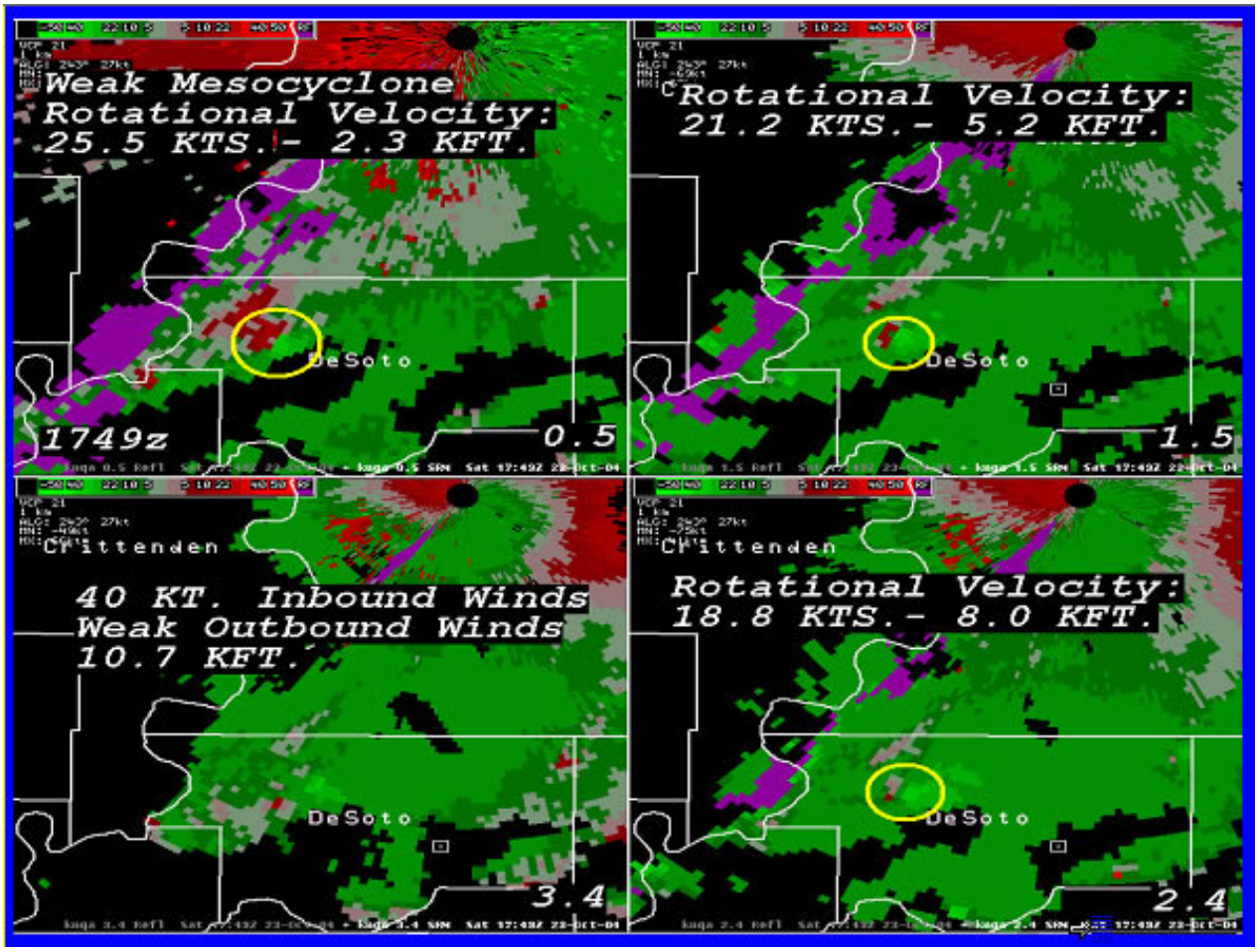

Figure 16b. Four panel display of Storm Relative Mean Velocity (SRM) at 1749 UTC, 23 October 2004. A weak but strengthening low level mesocyclone was noted in the lowest elevation slices. The strength of the mesocyclone at differing heights is indicated.

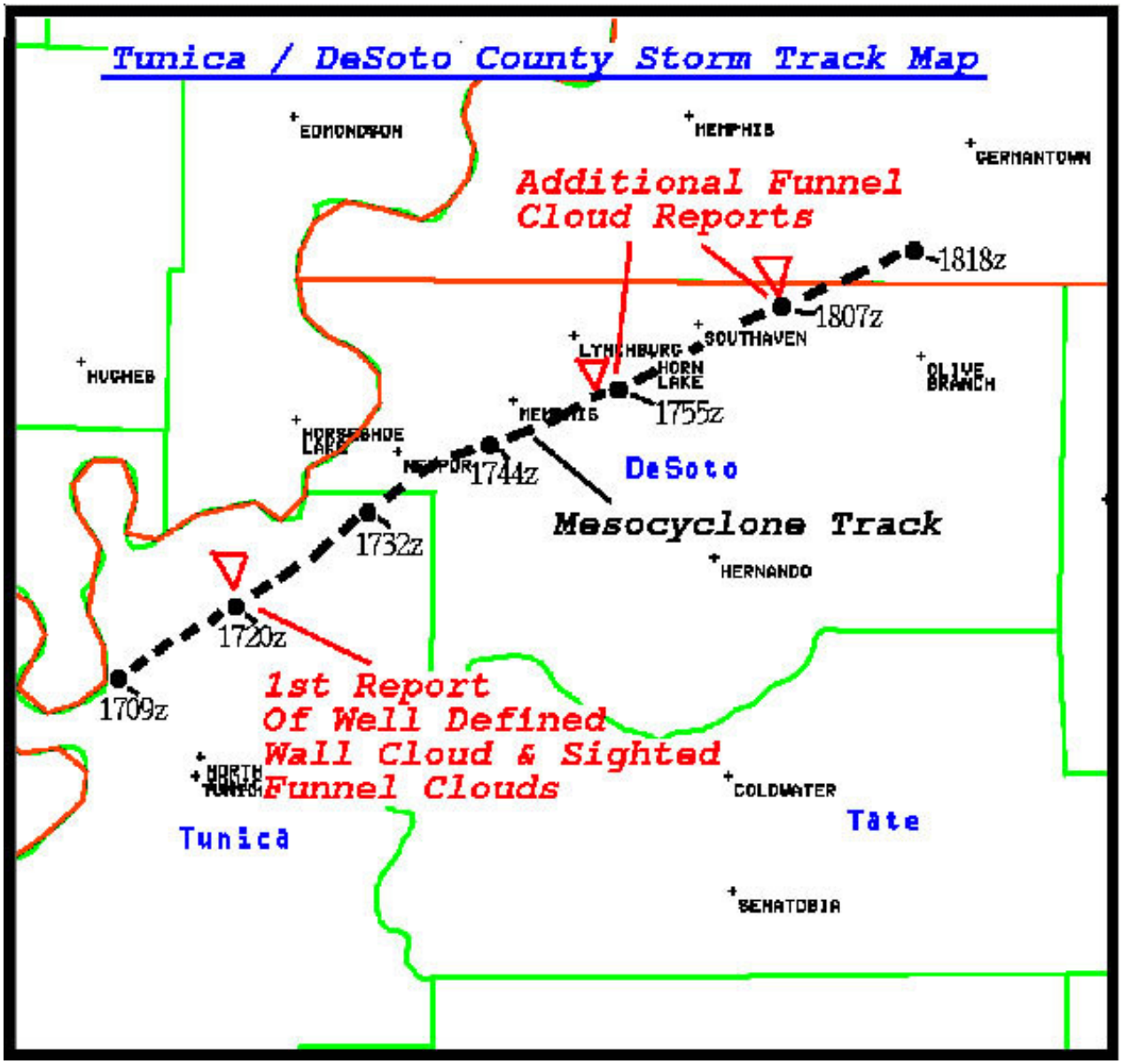

Figure 17. Track of Tunica/DeSoto County mini-supercell thunderstorm. The mesocyclone track is indicated by the dashed black line and reported funnel clouds are indicated by the red triangular symbols.

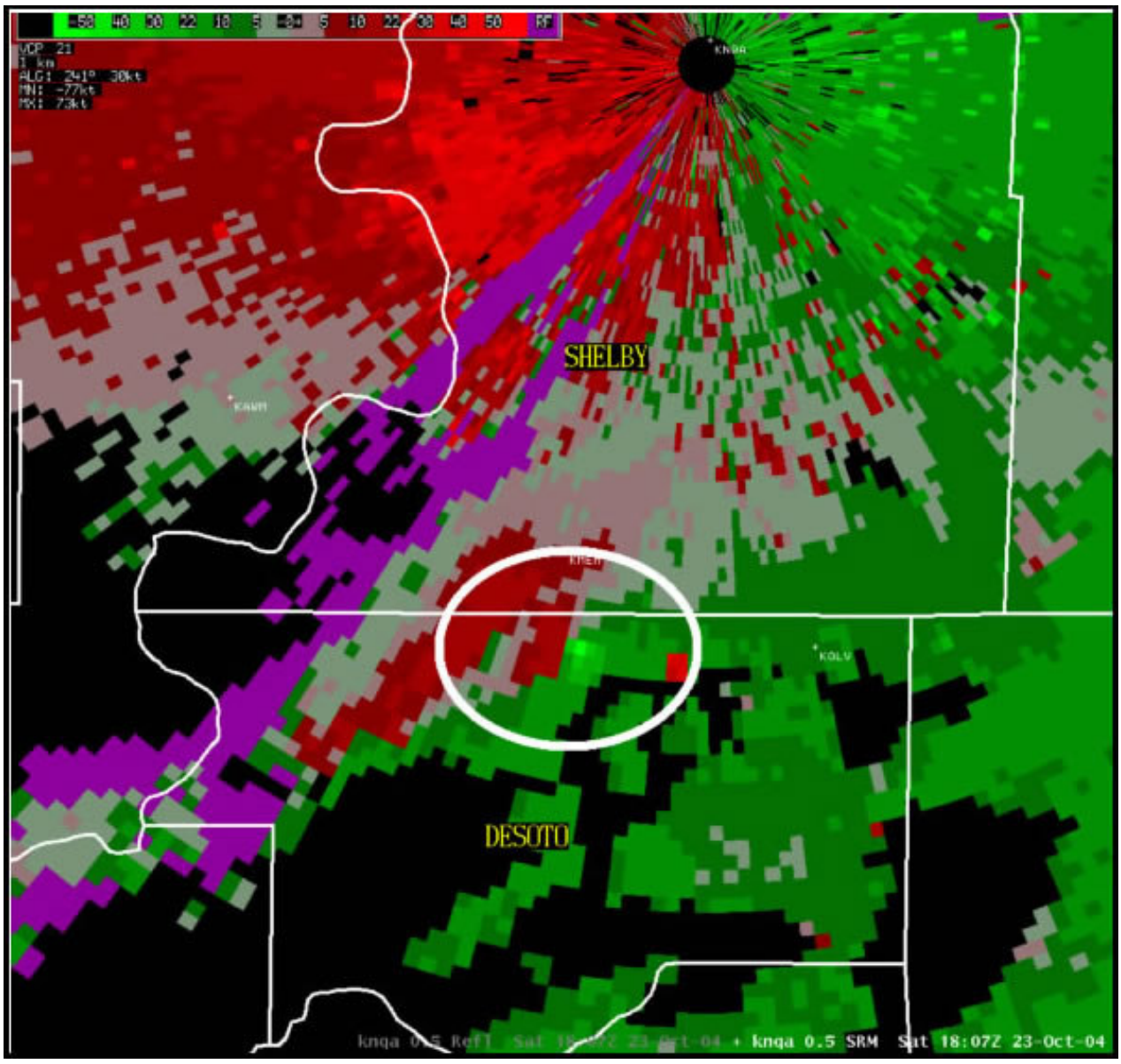

Figure 18a. 0.5 degree Strom Relative Mean Velocity (SRM) image from the KNQA WSR-88D at 1807 UTC, 23 October 2004. The low level mesocyclone reached maximum intensity at this time with rotational velocities measured in excess of 18 ms^{-1}.

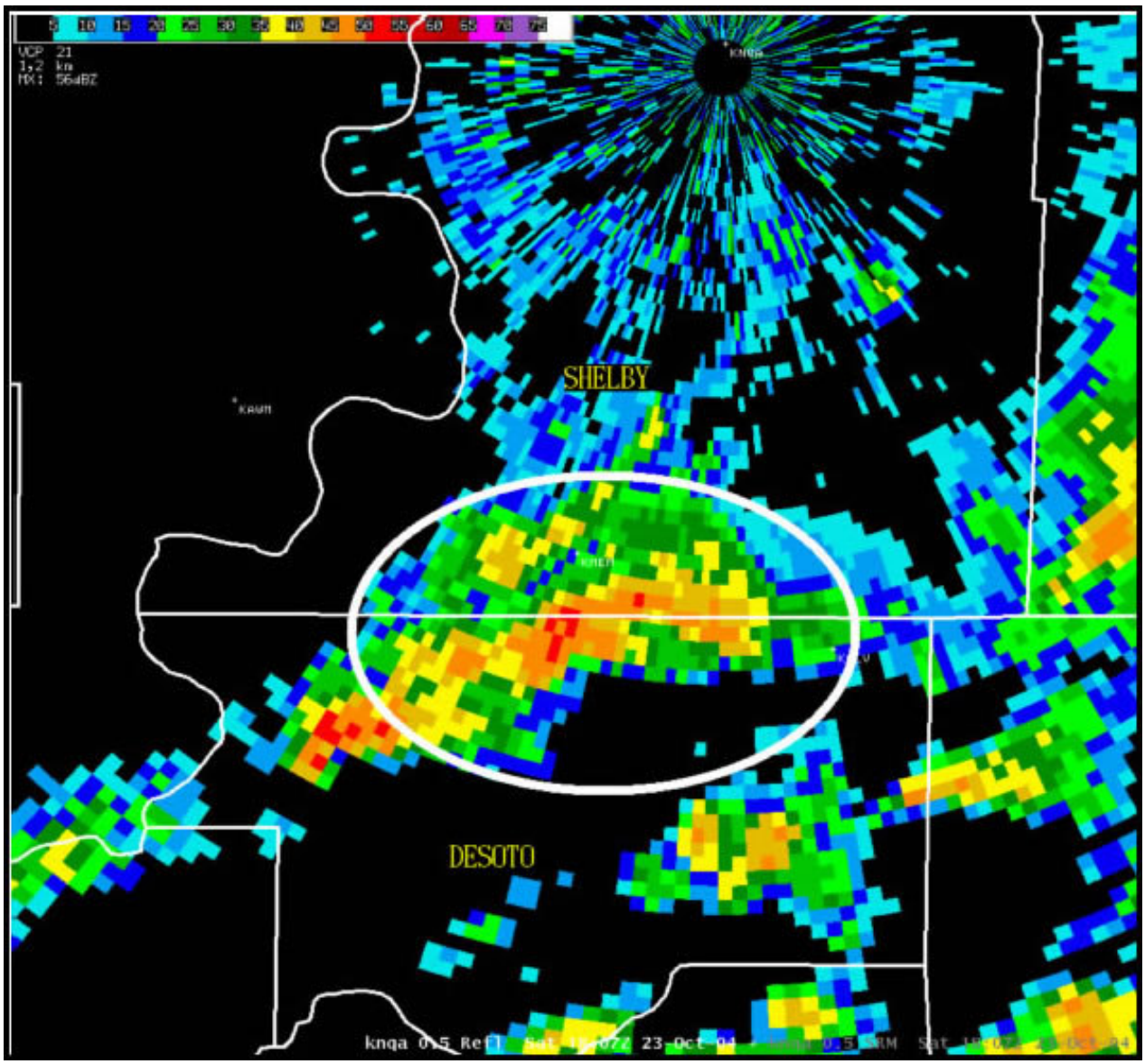

Figure 18b. 0.5 degree Base Reflectivity (BREF) image from the KNQA WSR-88D at 1807 UTC, 23 October 2004. Storm A was at maximum intensity and displayed a pronounced and persistent low level inflow notch and tight reflectivity gradient on the inflow side of the storm.

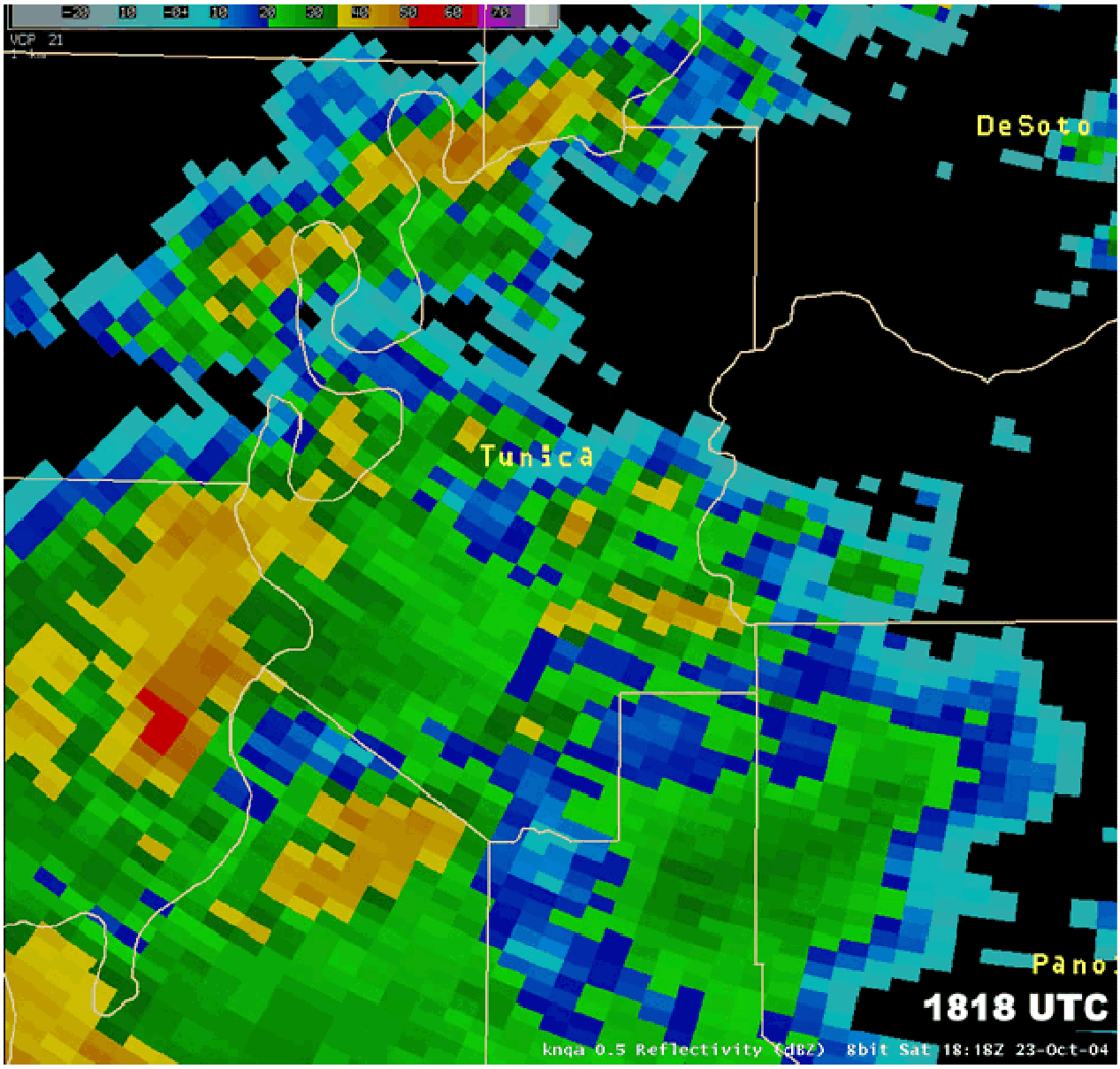

Figure 19a. 0.5 degree Base Reflectivity (BREF) loop from 1818 UTC to 1905 UTC. The BREF loop shows the interaction of Convective Outflow Boundary #2 with Storm B and the rapid development of Storm C.

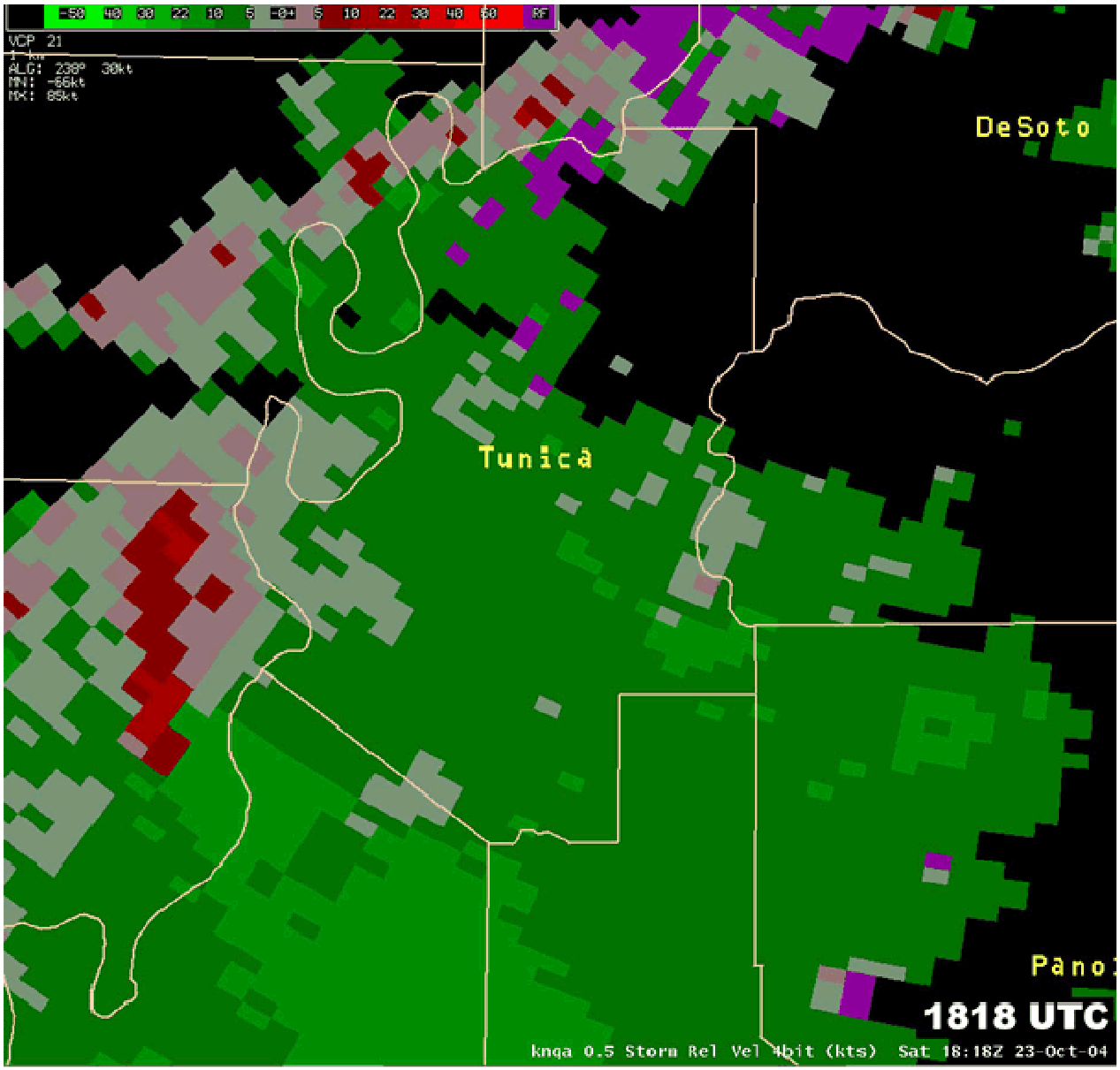

Figure 19b. 0.5 degree Storm Relative Mean Velocity (SRM) loop from 1818 UTC to 1905 UTC. The SRM loop shows the interaction of Convective Outflow Boundary #2 with Storm B and the rapid development of Storm C.

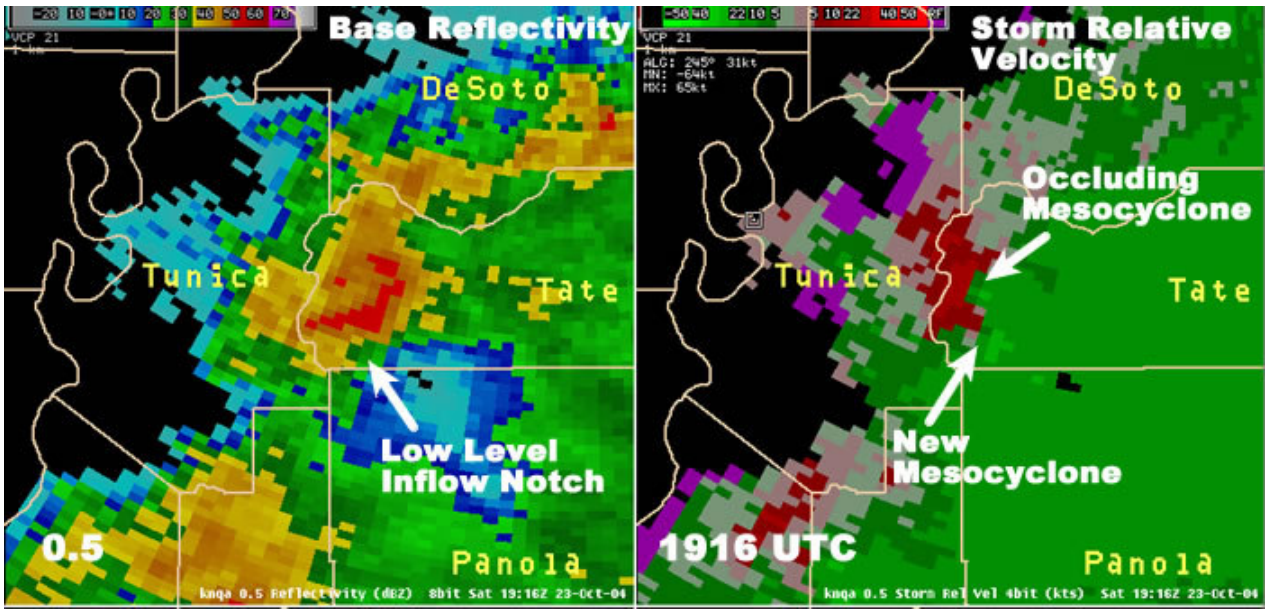

Figure 20. 0.5 degree Base Reflectivity (BREF) and Storm Relative Mean Velocity (SRM) at 1916 UTC showing the occlusion of the first low level mesocyclone in Storm C and the cyclical development of a new low level mesocyclone along the rear flank of the storm.

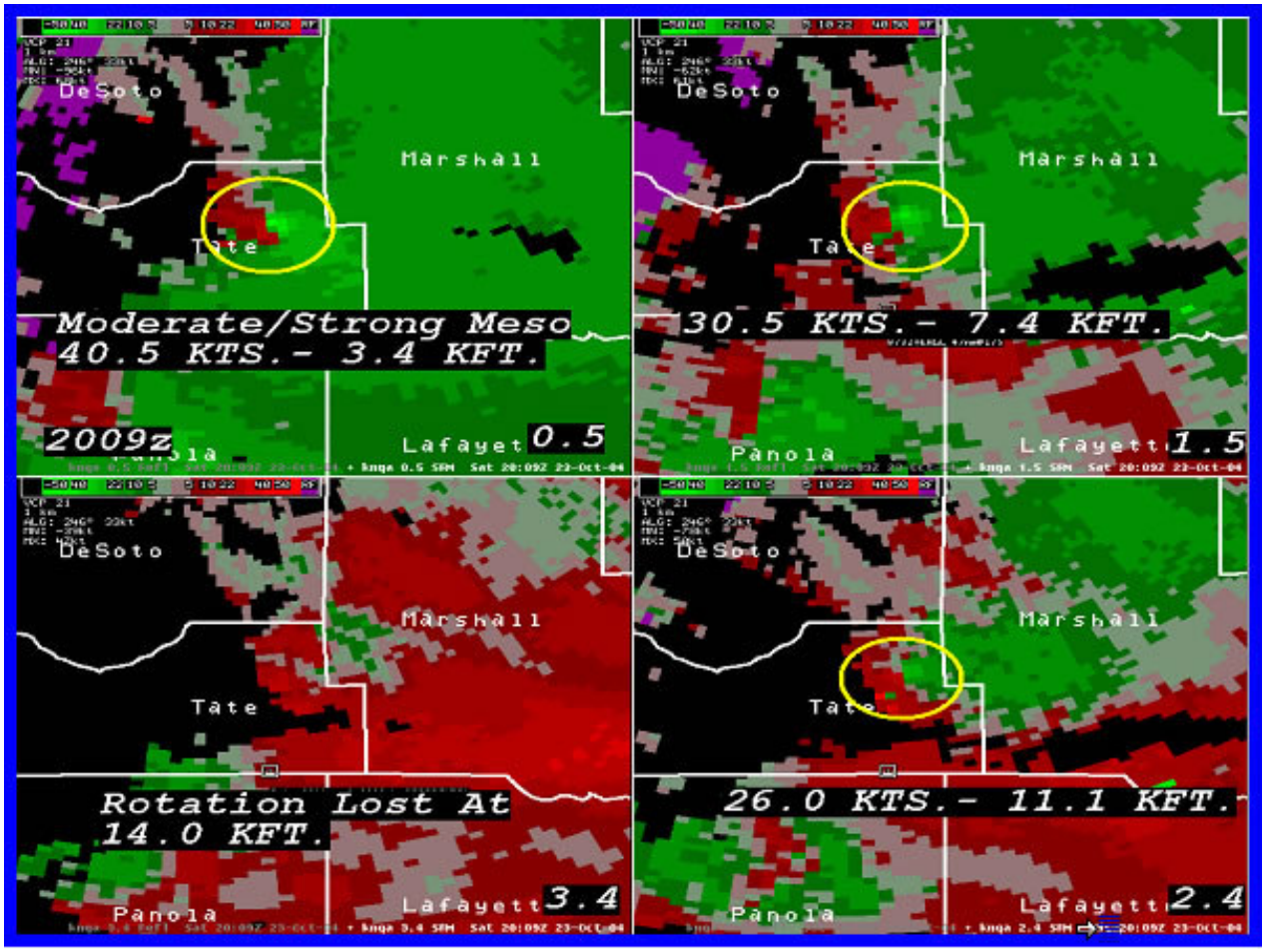

Figure 21a. Four panel Storm Relative Mean Velocity (SRM) from KNQA at 2009 UTC showing the low level mesocyclone restrengthening over Tate county, Mississippi. The strength of the mesocyclone at differing heights is indicated.

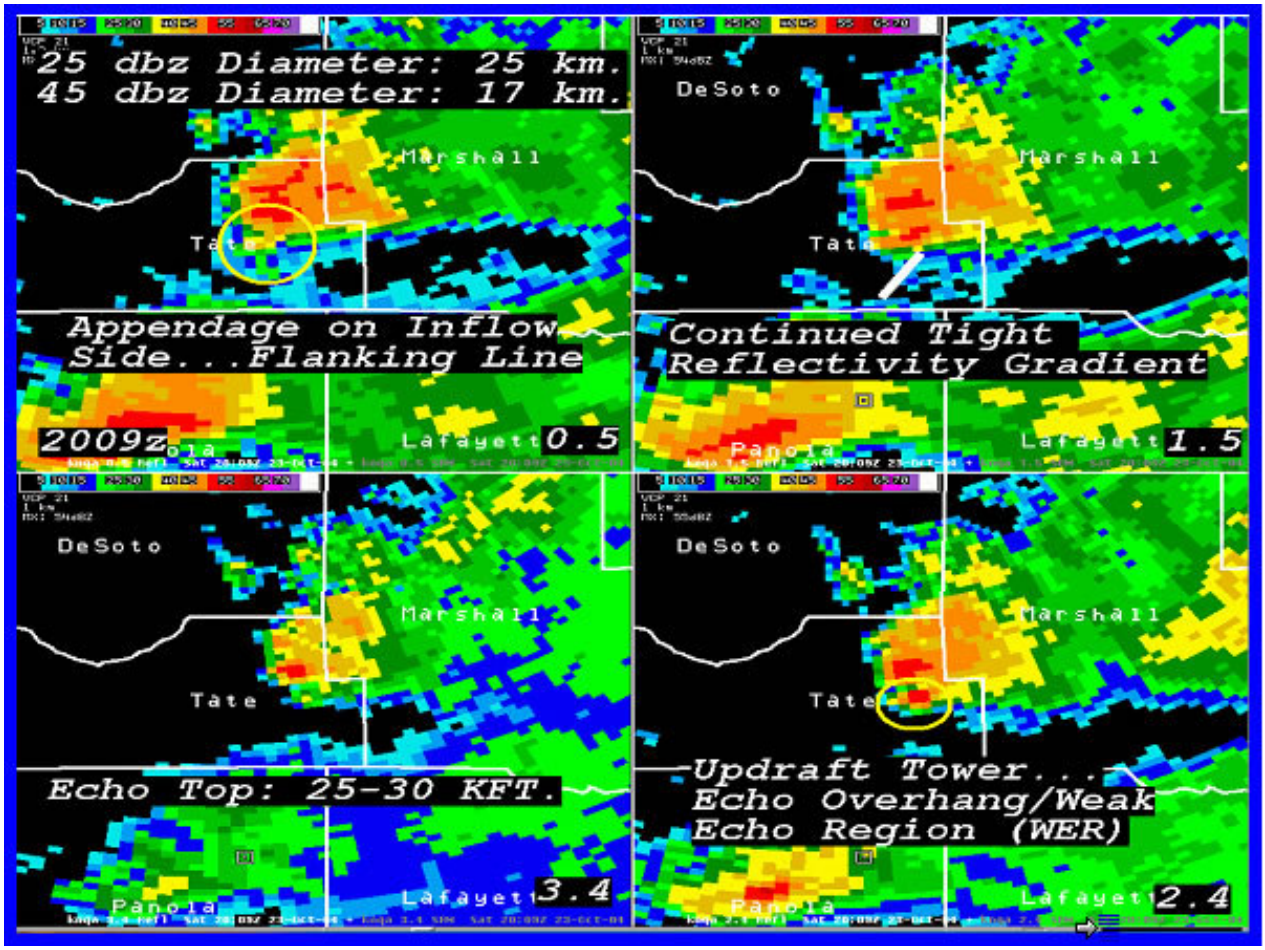

Figure 21b. Four panel Base Reflectivity (BREF) from KNQA at 2009 UTC showing the improved reflectivity structure of the mini-supercell thunderstorm a few minutes prior to producing the tornado of F1 intensity in Marshall County, Mississippi.

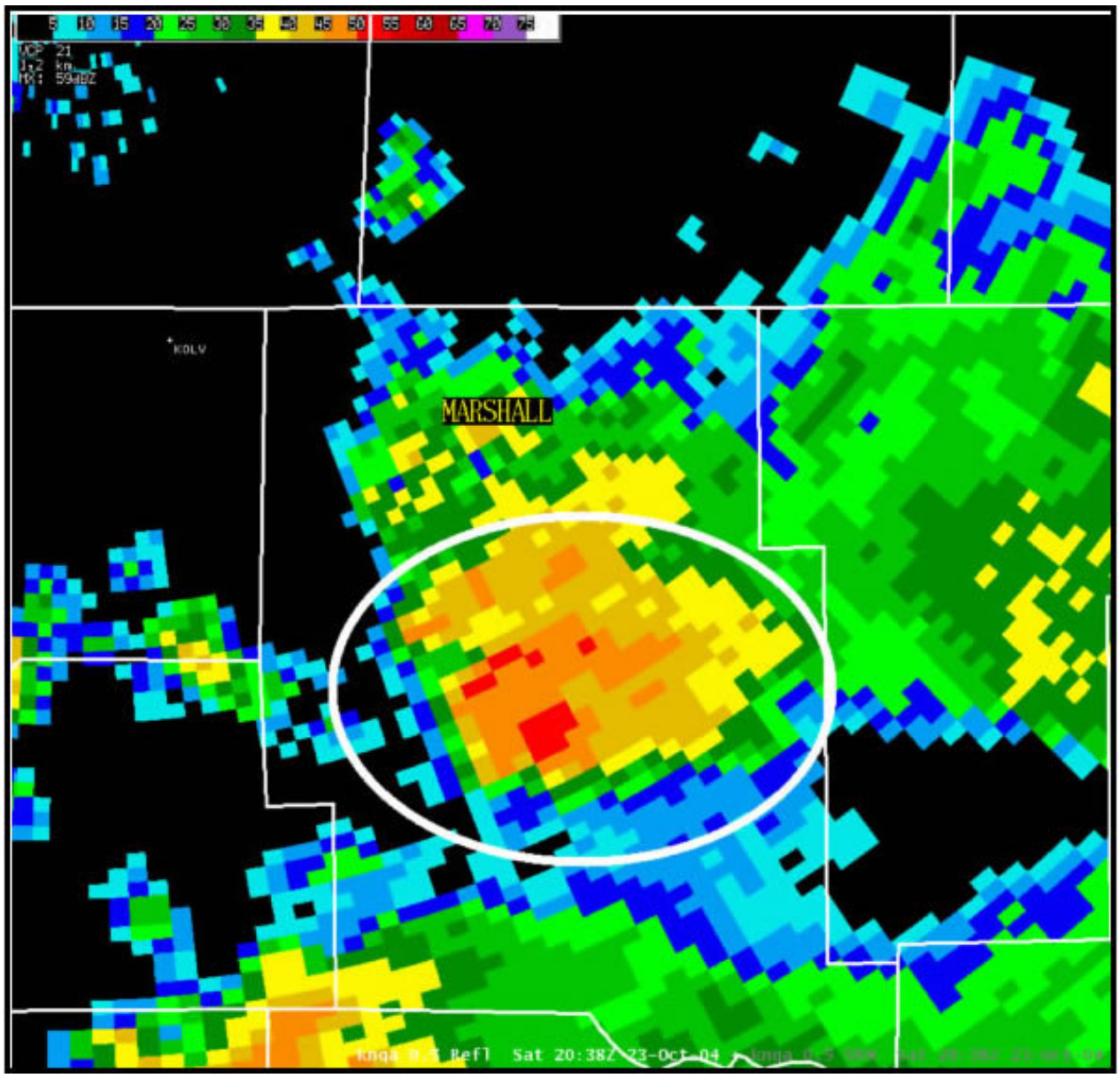

Figure 22a. 0.5 degree Base Reflectivity (BREF) image from the KNQA WSR-88D at 2038 UTC, 23 October 2004. At this time the reflectivity structure rapidly deteriorated as the thunderstorm collapsed. This occurred at the same time as tornadogenesis.

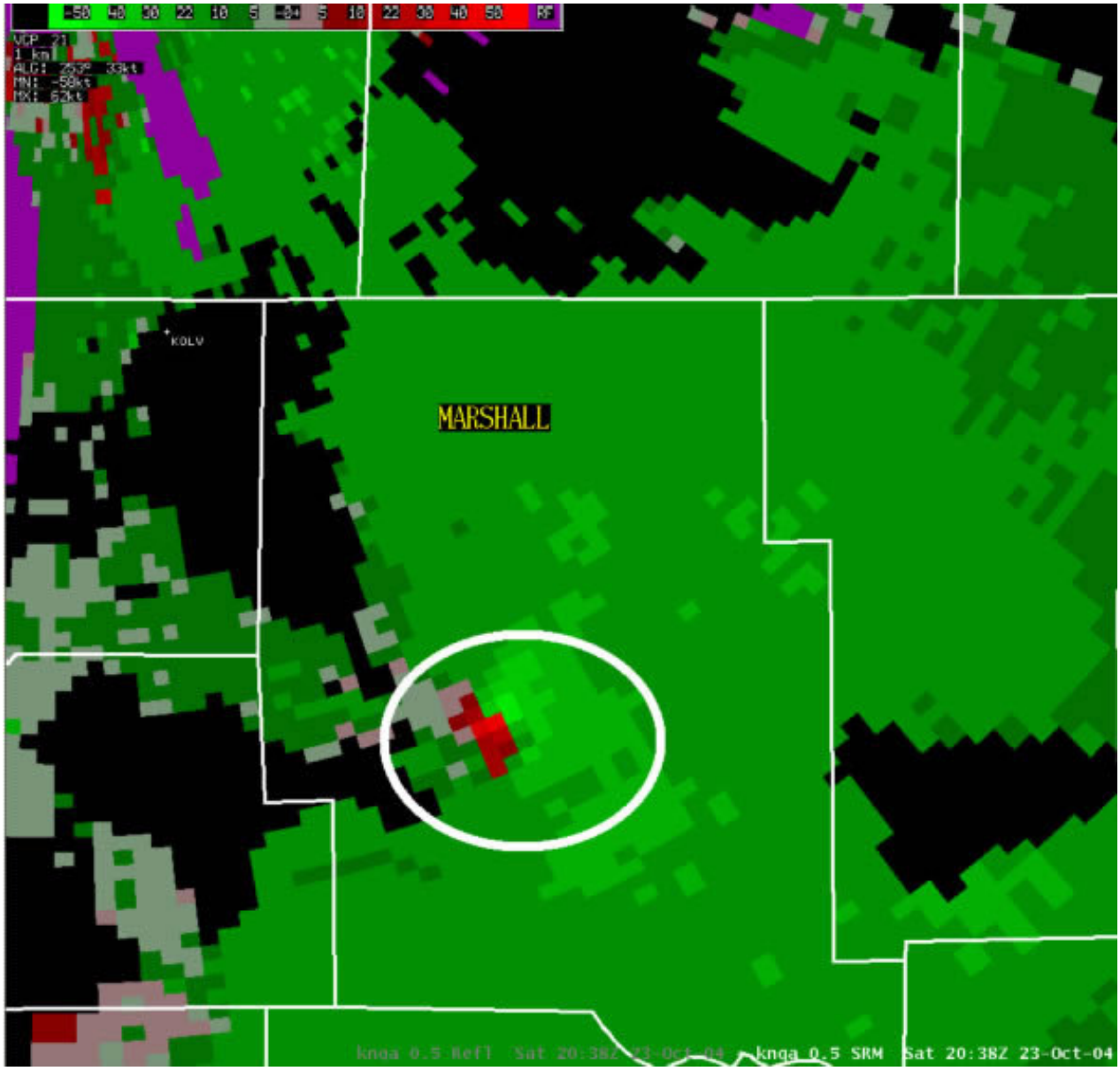

Figure 22b. 0.5 degree Storm Relative Mean Velocity (SRM) image from the KNQA WSR-88D at 2038 UTC, 23 October 2004. The low level mesocyclone had reached maximum intensity as the thunderstorm collapsed. It was at this time that the tornado was touching down in Marianna, Mississippi.

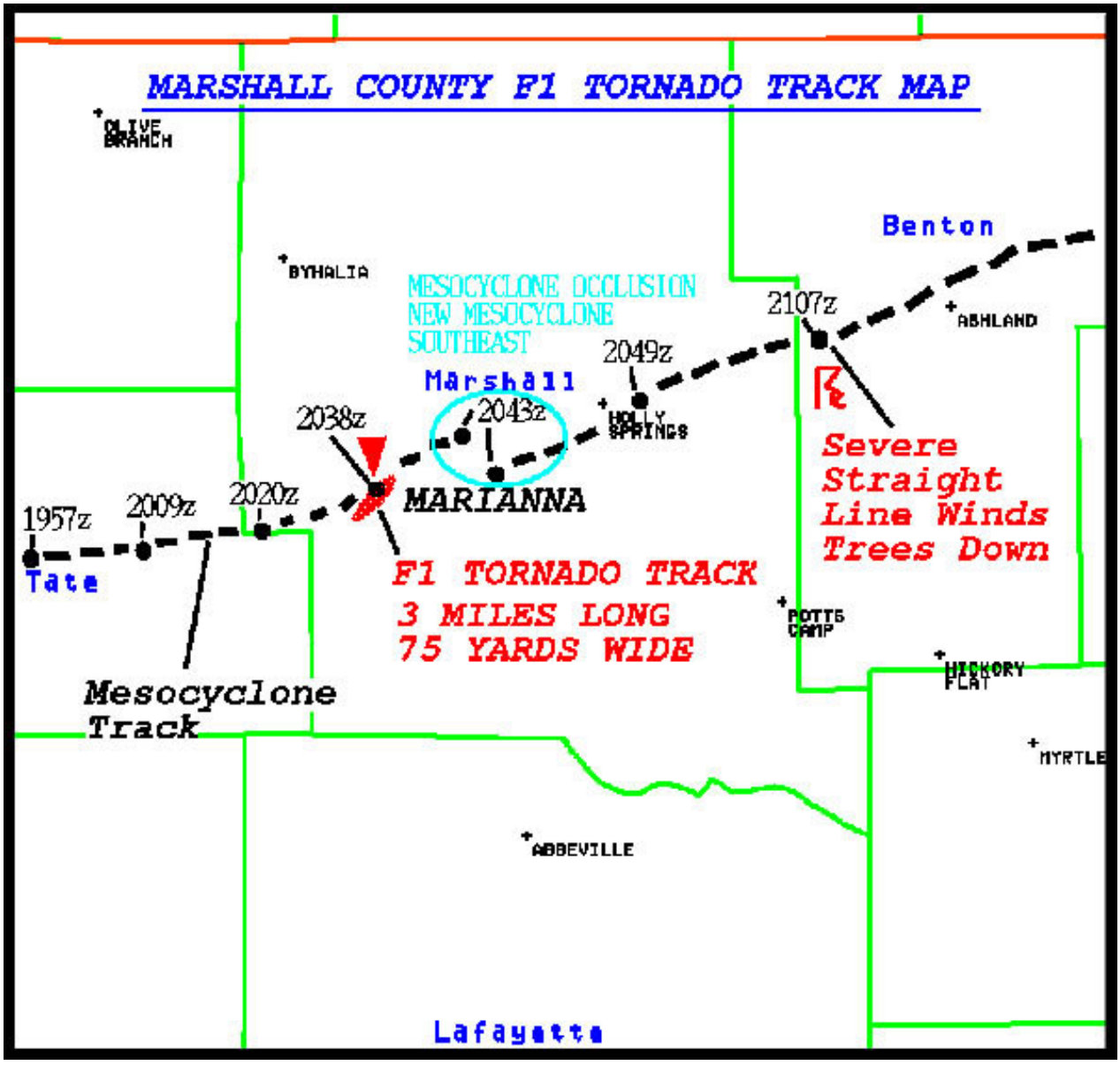

Figure 23. Track of the Marshall County Tornado (in red) that produced damage of F1 intensity. All of the damage associated with the tornado occurred within the city limits of Marianna, Mississippi.